

# ACE: ALL-ROUND CREATOR AND EDITOR FOLLOWING INSTRUCTIONS VIA DIFFUSION TRANSFORMER

Zhen Han\* Zeyinzi Jiang\* Yulin Pan\* Jingfeng Zhang\* Chaojie Mao\*†  
Chenwei Xie Yu Liu Jingren Zhou

Wanx Team Alibaba Group

## ABSTRACT

Diffusion models have emerged as a powerful generative technology and have been found to be applicable in various scenarios. Most existing foundational diffusion models are primarily designed for text-guided visual generation and do not support multi-modal conditions, which are essential for many visual editing tasks. This limitation prevents these foundational diffusion models from serving as a unified model in the field of visual generation, like GPT-4 in the natural language processing field. In this work, we propose ACE, an All-round Creator and Editor, which achieves comparable performance compared to those expert models in a wide range of visual generation tasks. To achieve this goal, we first introduce a unified condition format termed Long-context Condition Unit (LCU), and propose a novel Transformer-based diffusion model that uses LCU as input, aiming for joint training across various generation and editing tasks. Furthermore, we propose an efficient data collection approach to address the issue of the absence of available training data. It involves acquiring pairwise images with synthesis-based or clustering-based pipelines and supplying these pairs with accurate textual instructions by leveraging a fine-tuned multi-modal large language model. To comprehensively evaluate the performance of our model, we establish a benchmark of manually annotated pairs data across a variety of visual generation tasks. The extensive experimental results demonstrate the superiority of our model in visual generation fields. Thanks to the all-in-one capabilities of our model, we can easily build a multi-modal chat system that responds to any interactive request for image creation using a single model to serve as the backend, avoiding the cumbersome pipeline typically employed in visual agents. Code and models will be available on the project page: <https://ali-vilab.github.io/ace-page/>.

\*Equal Contribution. Order is determined by random dice rolling.

† Project leader and corresponding author.

# Table of Contents for ACE

<b>1</b>	<b>Introduction</b>	<b>3</b>
<b>2</b>	<b>All-Round Creator and Editor</b>	<b>4</b>
2.1	Problem Definition . . . . .	5
2.1.1	Tasks . . . . .	5
2.1.2	Input Paradigm . . . . .	6
2.2	Architecture . . . . .	6
<b>3</b>	<b>Datasets</b>	<b>7</b>
3.1	Pair Data Collection . . . . .	7
3.2	Instructions . . . . .	8
<b>4</b>	<b>Experiments</b>	<b>9</b>
4.1	Benchmarks and Metrics . . . . .	9
4.2	Qualitative Evaluation . . . . .	11
4.3	Quantitative Evaluation . . . . .	11
<b>5</b>	<b>Conclusion</b>	<b>12</b>
<b>A</b>	<b>Related Work</b>	<b>19</b>
<b>B</b>	<b>Datasets Detail</b>	<b>19</b>
B.1	Text-guided Generation . . . . .	19
B.2	Low-level Visual Analysis . . . . .	19
B.3	Controllable Generation . . . . .	21
B.4	Semantic Editing . . . . .	21
B.4.1	Facial Editing . . . . .	22
B.4.2	Style Editing . . . . .	23
B.4.3	General Editing . . . . .	23
B.5	Element Editing . . . . .	24
B.5.1	Text Editing . . . . .	25
B.5.2	Object Editing . . . . .	26
B.6	Repainting . . . . .	27
B.6.1	Unconditional Inpainting . . . . .	27
B.6.2	Text-guided Inpainting . . . . .	27
B.6.3	Outpainting . . . . .	28
B.7	Layer Editing . . . . .	28
B.8	Reference Generation . . . . .	29
B.8.1	Multi-reference Generation . . . . .	30
B.8.2	Reference-guided Editing . . . . .	30
B.9	Multi-turn and Long-context Generation . . . . .	30
<b>C</b>	<b>Benchmark Details</b>	<b>31</b>
<b>D</b>	<b>Implementation Details</b>	<b>32</b>
<b>E</b>	<b>More Experiments</b>	<b>32</b>
<b>F</b>	<b>Application</b>	<b>35</b>
F.1	Workflow Distillation . . . . .	35
F.2	Chat Bot . . . . .	35
<b>G</b>	<b>More Visualization</b>	<b>36</b>
<b>H</b>	<b>Discussion</b>	<b>36</b>



Figure 1: **Multi-turn image editing results of ACE.** ACE supports a wide range of image generation and editing tasks through natural language instructions, allowing complex and precise editing requests to be easily accomplished through multi-turn interactions.

## 1 INTRODUCTION

In recent years, foundational generative models have made groundbreaking progress in natural language processing (NLP) (Anil et al., 2023; Anthropic, 2023a;b; Ouyang et al., 2022). Conversational language models like ChatGPT (Brown et al., 2020; OpenAI, 2023b) offer a unified framework for addressing various NLP tasks through a prompt-guided approach. By employing a unified input-output structure, these models can achieve dynamic multi-turn interactions with users. Furthermore, by harnessing the knowledge of historical dialogues (Anthropic, 2024; OpenAI, 2024), they possess the capacity to comprehend intricate queries with greater nuance and depth. However, such unified architecture has not been fully explored in visual generation field. Existing foundational models of visual generation typically create images or videos from pure text, which is not compatible with most visual generation tasks, such as controllable image generation (Zhang et al., 2023b; Jiang et al., 2024) or image editing (Brooks et al., 2023). Thereby, specific visual generation tasks still require tailored tuning based on these foundational models, which is inflexible and inefficient. For this reason, the visual generative model has not yet become a powerful and unified productivity tool in various application scenarios like large language models (LLMs) (Abdin et al., 2024; Dubey et al., 2024; Bai et al., 2023; Yang et al., 2024).

One major challenge of building an all-in-one visual generation model lies in the diversity of multi-modal input formats and the variety of supported generation tasks. To address this, we design a unified framework using a Diffusion Transformer generation model that accommodates a wide range of inputs and tasks, empowering it to serve as an **All-round Creator and Editor**, which we refer to as **ACE**. First, we analyze the condition inputs of most visual generation tasks, and define Condition Unit (CU), which establishes a unified input paradigm consisting of core elements such as image, mask, and textual instruction. Second, for those CUs containing multiple images, we introduce Image Indicator Embedding to ensure the order of the images mentioned in instruction matches image sequence within the CUs. Besides, we imply 3d position embedding instead of 2d spatial-level position embedding on the image sequence, allowing for better exploring the relationships among conditional images. Third, we concatenate the current CU with historical information from previous generation rounds to construct the Long-context Condition Unit (LCU). By leveraging this chain of generation information, we expect the model to better understand the user’s request and create the desired image. As depicted in Fig. 1, ACE supports a range of generating and editing capabilities, allowing it to accomplish complex and precise generation tasks through multi-turn instructions.

To address the issue of the absence of available training data for various visual generation tasks, we establish a meticulous data collection and processing workflow to collect high-quality structured CU data at a scale of 0.7 billion. For visual conditions, we collect image pairs by synthesizing images from source images or by pairing images from large-scale databases. The former utilizes powerful open-source models to edit images to meet specific requirements, such as changing styles (Han et al., 2024) or adding objects (Pan et al., 2024), while the latter involves clustering and grouping images from extensive databases to provide sufficient real data, thereby minimizing the risk of overfitting to the synthesized data distribution. For textual instructions, we first manually construct instructions for diverse tasks by building templates or requesting LLMs, then optimize the instruction construction process by training an end-to-end instruction-labeling multi-modal large language model (MLLM) (Chen et al., 2024), thereby enriching the diversity of the text instructions.

Our ACE provides more comprehensive coverage of tasks on a single model compared to previous approaches. Therefore, to thoroughly evaluate the performance of our generation model, we construct an evaluation benchmark that encompasses the main tasks. This benchmark incorporates inputs sourced from both the real world and model-generated data, supporting global and local editing tasks. It is larger in scale and broader in scope compared to previous benchmarks (Sheynin et al., 2024; Zhang et al., 2023a). We conduct a user study to subjectively assess the quality of images generated by our method and the adherence to instructions, revealing that our approach generally aligns more closely with human perception across the majority of tasks. We summarize our main contributions as follows:

- We propose **ACE**, a unified foundational model framework that supports a wide range of visual generation tasks. To our knowledge, this is the most comprehensive diffusion generation model to date in terms of task coverage.
- By defining the CU for unifying multi-modal inputs across different tasks and incorporating long-context CU, we introduce historical contextual information into visual generation tasks, paving the way for ChatGPT-like dialog systems in visual generation.
- We design specific data construction pipelines for various tasks to enhance the quality and efficiency of data collection, and we ensure the richness of multi-modal data through MLLM fine-tuning for automated instruction labeling.
- We establish a more comprehensive evaluation benchmark compared to previous ones, covering the most known visual generation tasks. Evaluation results indicate that ACE demonstrates notable competitiveness in specialized models while also exhibiting strong generalization capabilities across a broader range of open tasks.

## 2 ALL-ROUND CREATOR AND EDITOR

ACE is an image creation and editing model based on the Diffusion Transformer that follows textual instructions. It establishes a unified framework that covers a wide range of tasks through the definition of standard input paradigm and strategy for aligning multi-modal information. With this



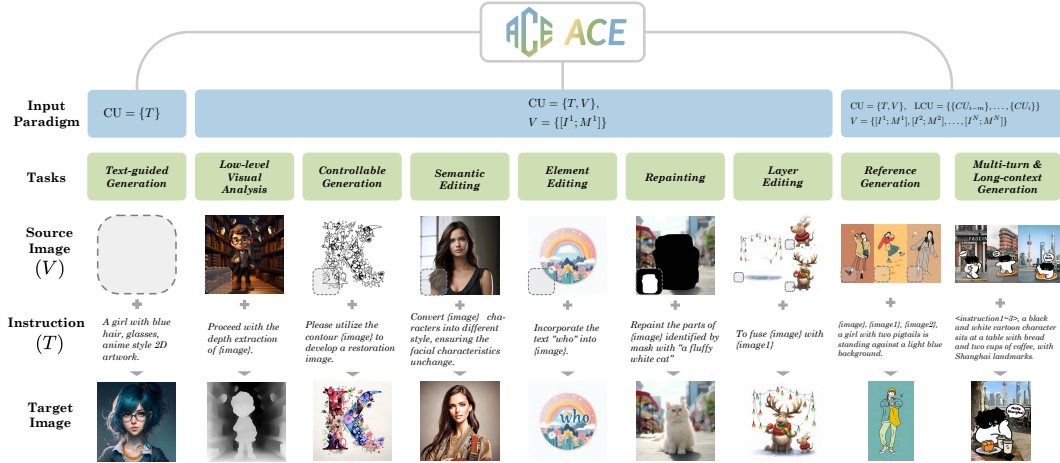


Figure 2: **The overview of all generation and editing task types supported by ACE.** These tasks are categorized into 8 basic types, multi-turn and long-context generation based on different input conditions (in green) and are formulated using the proposed input paradigm as 3 formats (in blue).

exquisite design, the model is capable of handling various single tasks, multi-turn tasks, and long-context tasks with historical information.

## 2.1 PROBLEM DEFINITION

### 2.1.1 TASKS

When it comes to generation and editing, the input condition information varies significantly depending on the specific task types. This encompasses a diverse range of forms, including textual instructions, conditioning images in controllable generation, masks used in region editing, and images in guided generation, among others. We analyze and categorize these conditions from textual and visual modalities respectively: **(i) Textual modality**: we refer to all types of textual conditions as instructions and categorize them into **Generating-based Instructions** and **Editing-based Instructions**, depending on whether they describe the content of the generated image directly or the difference from the input visual cues; **(ii) Visual modality**: we categorize all generation tasks into 8 basic types, as shown in Fig. 2.

- **Text-guided Generation.** It only uses generating-based text prompt as a condition to create images, and none of the visual cues are adopted.
- **Low-level Visual Analysis.** It extracts low-level visual features from input images, such as edge maps or segmentation maps. One source image and editing-based instruction are required in the task to accomplish creation.
- **Controllable Generation.** It is the inverse task of Low-level Visual Analysis, which creates vivid images based on given conditions, *e.g.*, edge map, contour image, doodle image, scribble image, depth map, segmentation map, low-resolution image, *etc.*
- **Semantic Editing.** It aims to modify some semantic attributes of an input image by providing editing instructions, such as altering the style of an image or modifying the facial attributes of a character.
- **Element Editing.** It focuses on adding, deleting, or replacing a specific subject in the image while keeping other elements unchanged.
- **Repainting.** It erases and repaints partial image content of input image indicated by given mask and instruction.
- **Layer Editing.** It decomposes an input image into different layers, each of which contains a subject or background, or reversely fuses different layers.
- **Reference Generation.** It generates an image based on one or more reference images, analyzing the common elements among them and presenting these elements in the generated image.

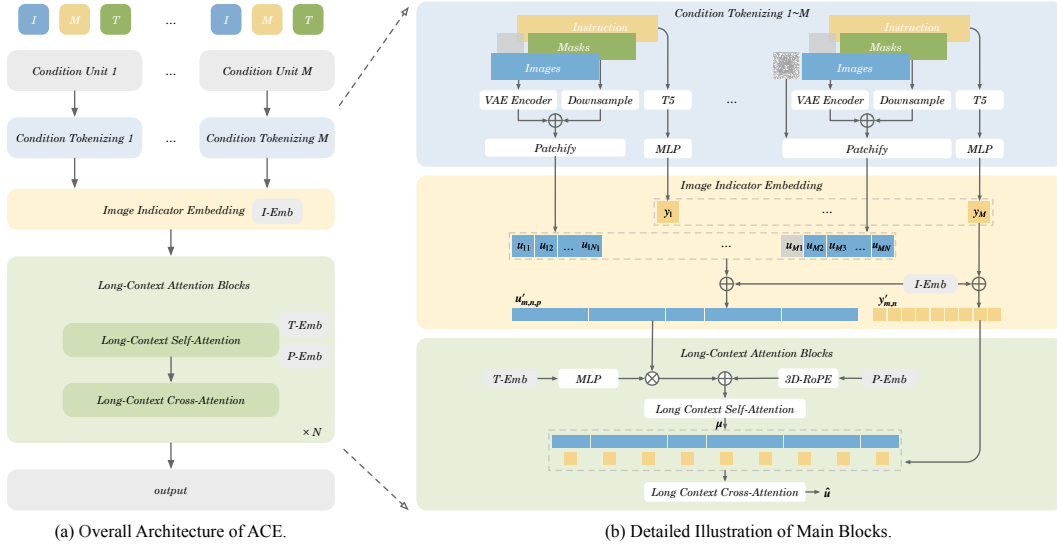


Figure 3: **The illustration of ACE framework.** Condition Tokenizing module tokenizes each input CU, concatenating them to obtain the visual token sequence and the text token sequence. The Image Indicator Embedding module employs pre-defined textual tokens to indicate the image order in textual instructions and distinguish various input images. The Long-context Attention Block ensures effective communication and integration of long-context sequences.

By leveraging the generation tasks of these fundamental units, we can combine them to create **multi-turn scenarios**. Furthermore, utilizing the historical information from every round makes it possible to tackle **long-context visual generation** tasks.

### 2.1.2 INPUT PARADIGM

A significant obstacle to implementing different types of generation and editing task requests within one framework lies in the diverse input condition formats of tasks. To address this issue, we design a unified input paradigm defined as Conditional Unit (CU) that fits as many tasks as possible. The CUs composed of a textual instruction  $T$  that describes the generation requirements, along with visual information  $V$ , where  $V$  consists of a set of images  $I$  that can be defined as  $I = \emptyset$  (if there are no source image) or  $I = \{I^1, I^2, \dots, I^N\}$  (if there are source images) and corresponding masks  $M = \{M^1, M^2, \dots, M^N\}$ . When there is no specific mask,  $M$  is set to a blank image. The overall formulation of the CU is as follows:

$$\text{CU} = \{T, V\}, \quad V = \{[I^1; M^1], [I^2; M^2], \dots, [I^N; M^N]\}, \quad (1)$$

where a channel-wise connection operation is performed between corresponding  $I$  and  $M$ ,  $N$  represents the total number of visual information inputs for this task.

Furthermore, to better address the demands of complex long-context generation and editing, historical information can be optionally integrated into CU, which is formulated as:

$$\text{LCU}_i = \{\{T_{i-m}, T_{i-m+1}, \dots, T_i\}, \{V_{i-m}, V_{i-m+1}, \dots, V_i\}\} \quad (2)$$

where  $m$  denotes the maximum number of rounds of historical knowledge introduced in the current request.  $\text{LCU}_i$  is a Long-context Condition Unit used to generate desired content for the  $i$ -th request.

## 2.2 ARCHITECTURE

In this section, we introduce a unified visual generation framework that can perform all visual generation tasks within a single model, and incorporate long-context conditions to enhance comprehension. As illustrated in Fig. 3a, the overall framework is built based on a Diffusion Transformer model (Vaswani et al., 2017; Peebles & Xie, 2023), and integrated with three novel components to achieve unified generation: Condition Tokenizing, Image Indicator Embedding, and Long-context Attention Block. We will provide a detailed description of them below.

**Condition Tokenizing.** Considering an LCU that comprises  $M$  CUs, the model involves three entry points for each CU: a language model (T5) (Raffel et al., 2020) to encode textual instructions, a Variational Autoencoder (VAE) (Kingma & Welling, 2014) to compress reference image to latent representation, and a down-sampling module to resize mask to the shape of corresponding latent image. The latent image and its mask (an all-one mask if no mask is provided) are concatenated along the channel dimension. These image-mask pairs are then patchified into 1-dimensional visual token sequences  $u_{m,n,p}$ , where  $m, n$  are indexes for CUs and visual information Vs in each CU, while  $p$  denotes the spatial index in patchified latent images. Similarly, textual instructions are encoded into 1-dimensional token sequences  $y_m$ . After processing within each CU, we separately concatenate all visual token sequences and all textual token sequences to form a long-context sequence.

**Image Indicator Embedding.** As illustrated as Fig. 3b, to indicate the image order in textual instructions and distinguish various input images, we encode some pre-defined textual tokens “{image}, {image1}, ..., {imageN}” into T5 embeddings as Image Indicator Embeddings ( $I$ -Emb). These indicator embeddings are added to the corresponding image embedding sequence and text embedding sequence, which is formulated as:

$$y'_{m,n} = y_m + I\text{-Emb}_{m,n}, \tag{3}$$

$$u'_{m,n,p} = u_{m,n,p} + I\text{-Emb}_{m,n}. \tag{4}$$

In this way, image indicator tokens in textual instructions and the corresponding images are implicitly associated.

**Long-context Attention Block.** Given the long-context visual sequence, we first modulate it with the time step embedding ( $T$ -Emb), then incorporate a 3D Rotational Positional Encodings (RoPE) (Su et al., 2023) to differentiate between different spatial- and frame-level image embeddings. During the Long Context Self-Attention, all image embeddings of each CU at each spatial location, are equivalently and comprehensively interact with each other by  $\mu = \text{Attn}(u', u')$ . Next, unlike the cross-attention layer of the conventional Diffusion Transformer model, where each visual token attends to all of the textual tokens, we implement cross-attention operation with each condition unit. That means image tokens in  $m$ -th CU will only attend to the textual tokens from the same CU. This can be formulated as:

$$\hat{u}_{m,n} = \text{Attn}(\mu_{m,n}, y'_{m,n}). \tag{5}$$

This ensures that, within the cross-attention layer, the text embeddings and image embeddings align on a frame-by-frame basis.

### 3 DATASETS

#### 3.1 PAIR DATA COLLECTION

A critical challenge of training foundational visual generation model lies in how to acquire pairwise images for various tasks. In this section, we introduce two ways to efficiently build high-quality datasets for most of the generation and editing tasks: **(i) Synthesizing from source image:** thanks to the rapid development in the field of visual generation, there have been many of powerful open-source models designed to solve one specific problem. Leveraging these powerful single-point technologies, we could synthesis plenty of image pairs for lots of generation and editing tasks, such as controllable generation, style editing, object editing, and so on. **(ii) Pairing from massive databases:** though the synthesis-based method is efficient and straightforward in acquiring pairwise data. However, It still possesses two drawbacks. First, some editing problems have not been fully explored, and there are no powerful open-source models available for these tasks. Second, using only synthetic data can easily cause over-fitting and reduce the quality of generated images. Therefore, it is essential to provide sufficient real data to address the aforementioned drawbacks. We propose a hierarchically aggregating pipeline for pairing content-related images from massive databases to build pairs of data for training, as illustrated in Fig. 4. We first extract semantic features using SigLIP (Zhai et al., 2023) from large-scale datasets (e.g., LAION-5B (Schuhmann et al., 2022), OpenImages (OpenImage, 2023), and our private datasets). Then leveraging K-means clustering technology, coarse-grained clustering is implemented to divide all images into tens of thousands of clusters. Within each cluster, we implement a two-turn union-find algorithm to achieve fine-grained

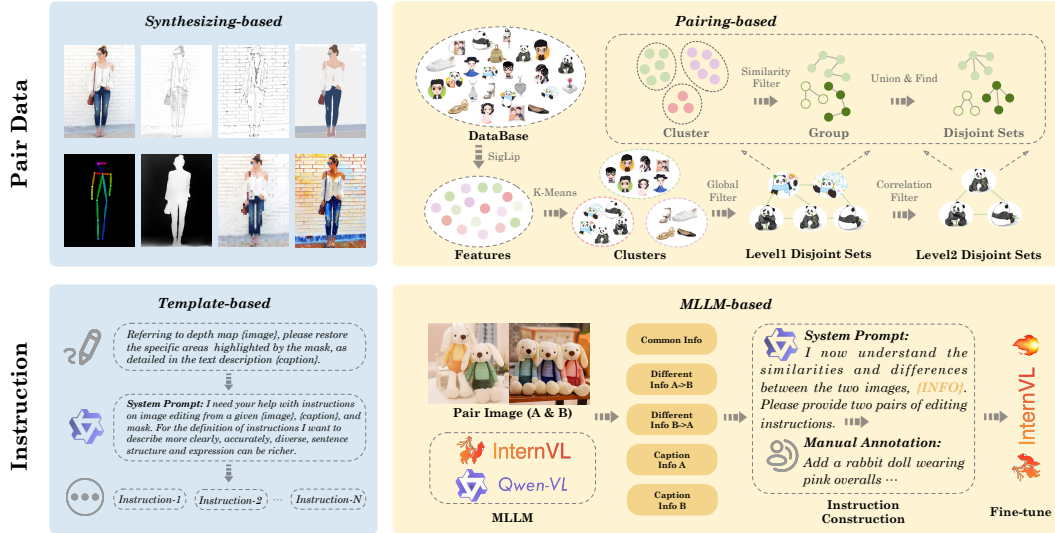


Figure 4: **The pipeline of dataset construction and instructions labeling.** In data construction, two methods are utilized: synthesizing using open-source expert models and mining from large-scale data. For instruction labeling, we combined templating with MLLM labeling, further training the Instruction Captioner to achieve large-scale instruction labeling.

image aggregation. The first turn is based on the SigLIP feature and the second turn uses a similarity score tailored for specific tasks. For instance, we calculate the face similarity score for the facial editing task and the object consistency score for the general editing task. Finally, we collect all possible pairs from each disjoint set and implement cleaning strategies to filter high-quality pairs. Benefiting from these two automatic pipelines, we construct a large-scale training dataset that consists of nearly 0.7 billion image pairs, covering 8 basic types of tasks, multi-turn and long-context generation. We depict its distribution in Fig. 6 and provide a detailed description of the specific data construction methods for each task, please refer to appendix B.

### 3.2 INSTRUCTIONS

In addition to collecting image pairs, it is essential to label clear natural language instructions that indicate how to transform one image into another. Compared to the caption generation commonly used in text-to-image task, instruction labeling is generally more challenging, as it requires analyzing not only the semantics of individual images, but also the discrepancies across multiple images. We employ both **Template-based** and **MLLM-based** methods to tackle this challenge. Template-based method constructs instruction templates for specific vision tasks by leveraging human knowledge priors. However, the instructions generated by this method lack diversity, which can lead to significant overfitting problems. MLLM-based method generates unique instructions for each given editing pair, leveraging off-the-shelf MLLMs. Nonetheless, current MLLMs exhibit limitations in producing precise instructions for editing tasks involving non-natural images, such as depth-controlled image generation and image segmentation. Thus, we combine these two methods and design an effective strategy to mitigate the aforementioned drawbacks. For tasks that contain non-natural images, we utilize a template-based method to generate instruction templates. These templates are then combined with the generated captions to produce the final instructions. To address the issue of insufficient diversity, we employ LLMs to reformulate instructions multiple times, and tune prompts to ensure that each rewritten version is distinct from all preceding instructions. For tasks that contain natural images, we employ an MLLM to predict the differences and commonalities between the images in the input pair. Then an LLM is used to generate instructions focusing on semantic distinctions according to the analysis of the differences and commonalities. Further, the collected instructions generated by these two methods undergo human annotation and correction. The revised instructions are used for fine-tuning an open-source MLLM, enabling it to predict instructions for any given image pair. Specifically, we collect a dataset of approximately 800,000 curated instructions and train an **Instruction Captioner** by fine-tuning the InternVL2-26B (Chen et al., 2024).

Table 1: **Results on the MagicBrush benchmark.** LC denotes long-context generation with history.

Settings	Methods	L1↓	L2↓	CLIP-I↑	DINO↑	CLIP-T↑	
Single-turn	<i>Global Description-guided</i>						
	SD-SDEdit (Meng et al., 2021)	0.1014	0.0278	0.8526	0.7726	0.2777	
	Null Text Inversion (Mokady et al., 2022)	0.0749	0.0197	0.8827	0.8206	0.2737	
	GLIDE (Nichol et al., 2022)	3.4973	115.8347	<b>0.9487</b>	<b>0.9206</b>	0.2249	
	Blended Diffusion (Avrahami et al., 2022)	3.5631	119.2813	0.9291	0.8644	0.2622	
	<b>ACE (Ours)</b>	<b>0.0505</b>	<b>0.0160</b>	<b>0.9436</b>	<b>0.9184</b>	<b>0.2833</b>	
	<i>Instruction-guided</i>						
	HIVE (Zhang et al., 2024)	0.1092	0.0380	0.8519	0.7500	-	
	InstructPix2Pix (Brooks et al., 2023)	0.1122	0.0371	0.8524	0.7428	0.2764	
	MagicBrush (Zhang et al., 2023a)	0.0625	0.0203	0.9332	0.8987	0.2781	
	UltraEdit (Zhao et al., 2024)	0.0575	0.0172	0.9307	0.8982	-	
	<b>ACE (Ours)</b>	<b>0.0507</b>	<b>0.0165</b>	<b>0.9453</b>	<b>0.9215</b>	<b>0.2841</b>	
	Multi-turn	<i>Global Description-guided</i>					
		SD-SDEdit (Meng et al., 2021)	0.1616	0.0602	0.7933	0.6212	0.2694
Null Text Inversion (Mokady et al., 2022)		0.1057	0.0335	0.8468	0.7529	0.2710	
GLIDE (Nichol et al., 2022)		11.7487	1079.5997	0.9094	0.8494	0.2252	
Blended Diffusion (Avrahami et al., 2022)		14.5439	1510.2271	0.8782	0.7690	0.2619	
<b>ACE (Ours)</b>		<b>0.0778</b>	<b>0.0290</b>	<b>0.9124</b>	<b>0.8611</b>	<b>0.2843</b>	
<b>ACE (Ours w/ LC)</b>		<b>0.0768</b>	<b>0.0285</b>	<b>0.9136</b>	<b>0.8635</b>	<b>0.2819</b>	
<i>Instruction-guided</i>							
HIVE (Zhang et al., 2024)		0.1521	0.0557	0.8004	0.6463	0.2673	
InstructPix2Pix (Brooks et al., 2023)		0.1584	0.0598	0.7924	0.6177	0.2726	
MagicBrush (Zhang et al., 2023a)		0.0964	0.0353	0.8924	0.8273	0.2754	
UltraEdit (Zhao et al., 2024)		<b>0.0745</b>	<b>0.0236</b>	0.9045	0.8505	-	
<b>ACE (Ours)</b>		0.0773	0.0293	<b>0.9128</b>	<b>0.8661</b>	<b>0.2855</b>	
<b>ACE (Ours w/ LC)</b>		0.0761	0.0284	<b>0.9140</b>	<b>0.8668</b>	0.2809	

Once trained, the Instruction Captioner is able to take any two images as input and generates the instruction for transforming the source image to the target image. It can also be further extended to the processing of cluster data, by entering a set of images, obtaining the similarity description among images within the cluster, and the differences between each pair within the cluster. The above process is illustrated in Fig. 4.

## 4 EXPERIMENTS

### 4.1 BENCHMARKS AND METRICS

**Existing Benchmarks.** We first evaluate on the commonly used benchmark MagicBrush (Zhang et al., 2023a). It contains an overall 1,053 edit turns and 535 edit sessions for single-turn and multi-turn image editing respectively. It compares the output images with groundtruth images and the provided target text descriptions. Following the setting proposed in the MagicBrush benchmark, we calculate the L1 distance, L2 distance, CLIP (Radford et al., 2021) similarity, DINO (Liu et al., 2023a) similarity between the generated image and groundtruth image, and CLIP similarity between the generated image and textual prompt. We also evaluate the Emu Edit benchmark (Sheynin et al., 2024), please see appendix E for details.

**ACE Benchmark.** To thoroughly evaluate the performance of various visual generation tasks, we build a benchmark dataset that covers all types of tasks the aforementioned. ACE benchmark consists of both real and generated images. The real images are primarily sourced from the MS-COCO (Lin et al., 2014) dataset and the generated images are created by Midjourney (Midjourney, 2023), using prompts obtained from JourneyDB (Sun et al., 2023a). For each task type, we manually craft instructions and masks to closely resemble actual user input patterns, reaching a total of 12,000 entries. The detailed statistics of ACE benchmark can be found in Fig. 24. We evaluate image quality and prompt following scores through a user study. The image quality score assesses the aesthetic quality of the generated images, while the prompt following score measures how well the images align with the provided textual instructions.



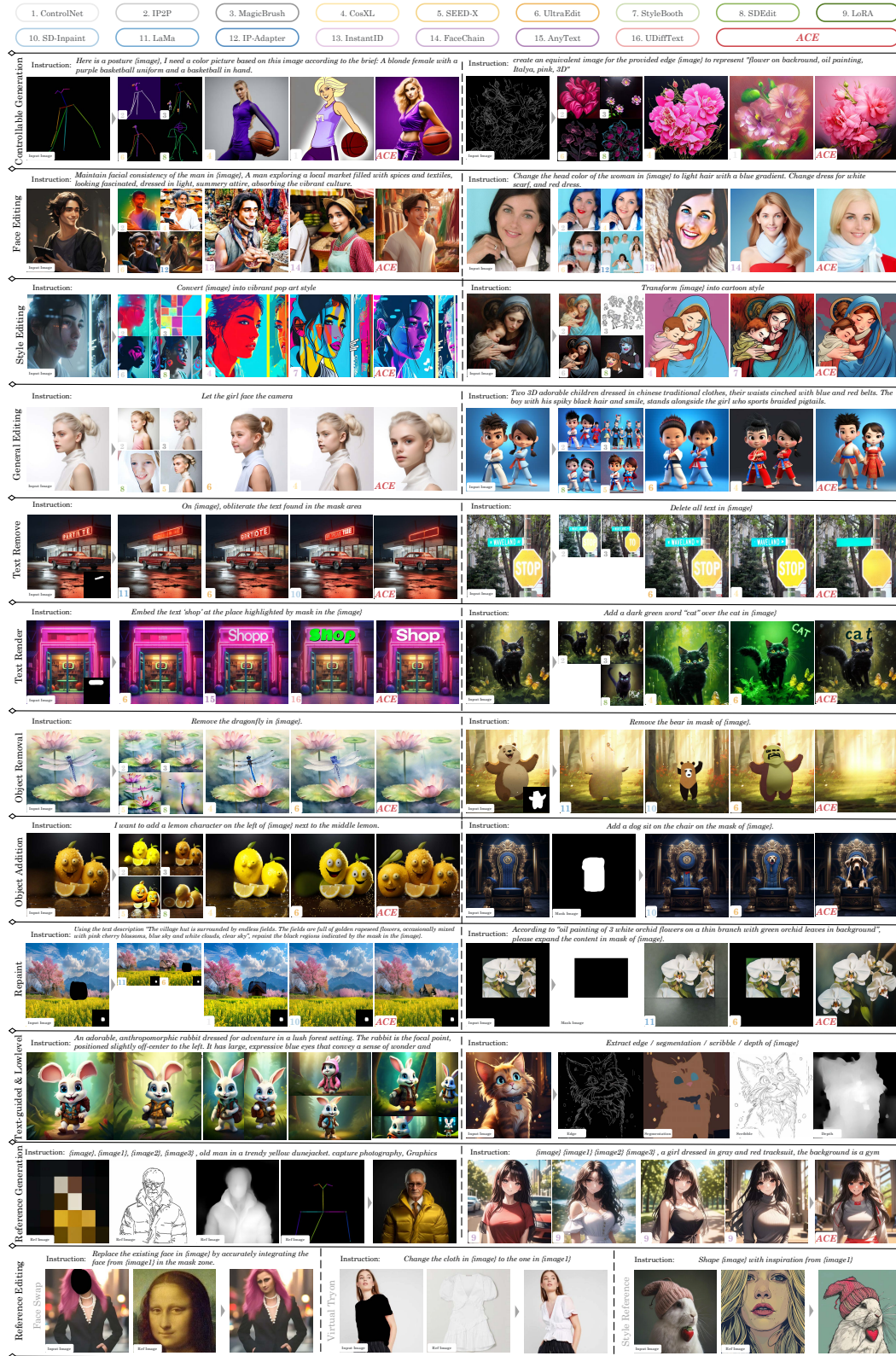


Figure 5: Comparison and visualization of ACE performance with expert models in different tasks. ACE demonstrates adaptability to multi-task and achieves superior performance.

Table 2: **User study results on ACE benchmark.** For each method in every supported task, we evaluate both prompt following and image quality, reporting the two scores in a single cell, separated by a “/”. “-” means this task does not exist or is not supported by the current method.

	Txt2img	Controllable				Semantic			Element				Repainting	
	Txt2img	Canny	Depth	Scribble	Pose	Face	Style	General	Add Text	Rm Text	Add Obj.	Rm Obj.	Inpaint	Outpaint
<i>Global Editing</i>														
SD1.5 (AI, 2022a)	3.3/2.2	-	-	-	-	-	-	-	-	-	-	-	-	-
SDXL (StabilityAI, 2022)	<b>4.1/2.8</b>	-	-	-	-	-	-	-	-	-	-	-	-	-
CtrlNet (Zhang et al., 2023b)	-	2.5/2.0	3.8/2.4	1.9/2.0	2.9/1.9	-	-	-	-	-	-	-	-	-
StyleBooth (Han et al., 2024)	-	-	-	-	-	-	<b>3.3/2.6</b>	-	-	-	-	-	-	-
IP-Adapter (Ye et al., 2023)	-	-	-	-	-	2.0/2.2	-	1.7/2.5	-	-	-	-	-	-
InstantID (Wang et al., 2024b)	-	-	-	-	-	2.5/2.7	-	-	-	-	-	-	-	-
FaceChain (Liu et al., 2023b)	-	-	-	-	-	2.0/3.0	-	-	-	-	-	-	-	-
SDEdit (Meng et al., 2021)	-	1.4/1.9	1.3/1.8	1.1/1.6	1.2/1.4	1.3/2.1	1.1/1.7	1.5/2.1	1.1/2.2	1.1/1.7	1.5/2.1	1.1/2.0	-	-
IP2P (Brooks et al., 2023)	-	1.9/2.0	1.7/2.0	1.5/2.3	1.4/1.4	2.3/2.4	2.4/2.5	2.2/2.4	1.1/2.6	1.3/2.6	2.0/2.4	1.5/2.4	-	-
MB (Zhang et al., 2023a)	-	1.3/1.8	1.3/1.7	1.3/1.9	1.1/1.3	2.4/2.3	1.4/2.0	2.2/2.3	1.5/2.4	2.2/2.5	3.1/2.2	2.1/2.4	-	-
SEED-X (Ge et al., 2024b)	-	1.6/2.1	1.7/2.0	1.7/2.2	1.5/1.5	2.0/2.7	2.2/2.5	2.1/2.7	1.3/2.6	2.1/2.6	1.9/2.6	2.5/2.4	-	-
CosXL (StabilityAI, 2024)	-	4.1/2.9	4.1/2.8	2.6/2.9	3.7/2.1	2.9/3.1	3.2/3.0	3.2/2.9	1.4/2.7	1.0/2.9	2.8/2.5	1.1/3.1	-	-
UltraEdit (Zhao et al., 2024)	-	1.7/2.2	1.2/1.8	1.3/2.3	1.1/1.3	2.3/2.5	2.1/2.4	2.6/2.5	1.7/2.6	1.1/2.7	2.7/2.3	1.5/2.6	-	-
<b>ACE (Ours)</b>	<b>3.7/2.5</b>	<b>4.6/2.7</b>	<b>4.5/2.8</b>	<b>4.8/2.9</b>	<b>4.1/2.3</b>	<b>2.8/2.8</b>	<b>2.4/2.6</b>	<b>2.1/2.5</b>	<b>2.8/2.7</b>	<b>4.4/2.9</b>	<b>2.6/2.4</b>	<b>3.9/2.5</b>	-	-
<i>Local Editing</i>														
LaMa (Suvorov et al., 2022)	-	-	-	-	-	-	-	-	-	3.6/2.8	-	<b>4.5/2.8</b>	1.6/2.3	3.0/2.4
SDInpaint (AI, 2022b)	-	-	-	-	-	-	-	-	-	2.6/2.6	1.6/2.7	2.2/2.5	3.6/2.6	-
CtrlNet (Zhang et al., 2023b)	-	-	-	-	-	-	-	-	-	2.9/2.7	1.9/2.5	2.6/2.2	3.0/2.1	3.2/2.1
AnyText (Tuo et al., 2023)	-	-	-	-	-	-	-	-	3.5/2.7	-	-	-	-	-
UDiffText (Zhao & Lian, 2024)	-	-	-	-	-	-	-	-	3.6/2.7	-	-	-	-	-
UltraEdit (Zhao et al., 2024)	-	1.4/1.9	1.2/1.8	1.2/2.0	-	-	-	-	1.1/2.8	1.2/2.9	2.9/2.5	1.4/2.5	1.1/1.7	1.1/2.1
<b>ACE (Ours)</b>	-	<b>4.8/2.6</b>	<b>4.3/2.5</b>	<b>4.8/2.6</b>	-	-	-	-	<b>4.5/2.9</b>	<b>4.5/2.9</b>	<b>3.7/2.5</b>	<b>4.3/2.5</b>	<b>4.4/2.7</b>	<b>4.6/2.8</b>

## 4.2 QUALITATIVE EVALUATION

In our qualitative evaluation, we present a comparison of our method with SOTA approaches across various tasks, including ControlNet (Zhang et al., 2023b), InstructPix2Pix (Brooks et al., 2023), MagicBrush (Zhang et al., 2023a), CosXL (StabilityAI, 2024), SEED-X Edit (Ge et al., 2024a), UltraEdit (Zhao et al., 2024), StyleBooth (Han et al., 2024), SDEdit (Meng et al., 2021), LoRA (Hu et al., 2022), SD-Inpaint (AI, 2022b), LaMa (Suvorov et al., 2022), IP-Adapter (Ye et al., 2023), InstantID (Wang et al., 2024b), FaceChain (Liu et al., 2023b), AnyText (Tuo et al., 2023), UDiffText (Zhao & Lian, 2024). In Fig. 5, we present qualitative comparisons between our single ACE model and 16 other methods across 12 subtasks. Overall, our method not only addresses a diverse range of tasks but also performs superior compared to task-specific methods. Additionally, we also show some extra tasks that the comparison methods do not perform well in the last three lines. Please see appendix G, for more examples of qualitative evaluation.

## 4.3 QUANTITATIVE EVALUATION

**Evaluation on Existing Benchmarks.** We first compare our method with baselines on the MagicBrush benchmark. Results are present on Tab. 1. For single-turn image editing, ACE significantly outperforms other methods under an instruction-guided setting while demonstrating comparable performance under a description-guided setting. For each setting of multi-turn image editing, we first employ the same inference way as MagicBrush, performing independent and continuous edits on a single image. The results show that our approach has significant advantages. Furthermore, we construct a long sequence using the historical information from each editing round, achieving a certain improvement in performance compared to not using it. This also demonstrates the effectiveness of LCU and architecture design.

**Evaluation on ACE Benchmark.** We conduct a comprehensive human evaluation using our benchmark to assess the performance of generated images, employing image scoring as the evaluation metric. Specifically, we score each image considering two aspects: prompt following and image quality. The prompt following metric measures the image compliance with text instructions or text descriptions, and is categorized into five levels. The image quality metric encompasses various as-



pects such as generated color, details, layout, and visual appeal, and is scored on a scale from 1 to 5. Considering the broad capabilities of our method, we compare it with several common approaches and some experts designed for specific tasks. We engaged 5 professional designers as evaluators to carry out these assessments. For each task, the data is evenly distributed among the evaluators in an anonymous manner, and scores are aggregated for analysis.

As shown in Tab. 2, we compare our approach across multiple global editing tasks and local editing tasks. The prompt following score and image quality score are presented together, separated by a “/” pattern. The bold numbers represent the best, and the underlined numbers indicate the second best. Our method achieves the highest prompt following scores in 7 of 12 global editing tasks and 8 of 10 local editing tasks, which demonstrates that ACE fully understands the intention of the instruction and is able to correctly generate an image that meets the instruction. Furthermore, ACE achieves the best image quality scores in 5 of 10 global editing tasks and 7 of 10 local editing tasks. These results indicate that ACE excels at generating high aesthetic images across various image editing tasks. Nonetheless, our method performs unsatisfactorily in certain tasks, such as general editing and style editing. One possible reason is that images generated by methods using larger models, such as those producing 1024-resolution images based on the SDXL model, are more preferred by evaluators compared to those produced by our model, which has a size of 0.6B parameters and an output resolution of around 512.

## 5 CONCLUSION

We propose ACE, a versatile foundational generative model that excels at creating images, and following instructions across a wide range of generative tasks. Users can specify their generation intentions through customized text prompts and image inputs. Furthermore, we advance the exploration of capabilities within interactive dialogue scenarios, marking a significant step forward in the processing of long contextual historical information in the field of visual generation. Our work aims to provide a comprehensive generative model for the public and professional designers, serving as a productivity enhancement tool to foster innovation and creativity.

**Acknowledgments.** We sincerely appreciate the contributions of many colleagues for their insightful discussions, valuable suggestions, and constructive feedback, including: Haiming Zhao, Yuntao Hong, You Wu, Jixuan Chen, Yuwei Wang, and Sheng Yao for their data contributions, and Lianghua Huang, Kai Zhu, and Yutong Feng for their discussions, suggestions, and the sharing of resources.

## REFERENCES

- Marah Abdin, Jyoti Aneja, Hany Awadalla, Ahmed Awadallah, Ammar Ahmad Awan, Nguyen Bach, Amit Bahree, Arash Bakhtiari, Jianmin Bao, Harkirat Behl, Alon Benhaim, Misha Bilenko, Johan Bjorck, Sébastien Bubeck, et al. Phi-3 Technical Report: A Highly Capable Language Model Locally on Your Phone. *arXiv preprint arXiv:2404.14219*, 2024.
- Runway AI. Stable Diffusion v1.5 Model Card, <https://huggingface.co/runwayml/stable-diffusion-v1-5>, 2022a.
- Runway AI. Stable Diffusion Inpainting Model Card, <https://huggingface.co/runwayml/stable-diffusion-inpainting>, 2022b.
- Rohan Anil, Andrew M. Dai, Orhan Firat, Melvin Johnson, Dmitry Lepikhin, Alexandre Passos, et al. PaLM 2 Technical Report. *arXiv preprint arXiv:2305.10403*, 2023.
- Anthropic. Introducing Claude, <https://www.anthropic.com/index/introducing-claude>, 2023a.
- Anthropic. Claude 2. Technical report, <https://www-files.anthropic.com/production/images/Model-Card-Claude-2.pdf>, 2023b.
- Anthropic. The Claude 3 Model Family: Opus, Sonnet, Haiku, [https://www-cdn.anthropic.com/de8ba9b01c9ab7cbabf5c33b80b7bbc618857627/Model\\_Card\\_Claude\\_3.pdf](https://www-cdn.anthropic.com/de8ba9b01c9ab7cbabf5c33b80b7bbc618857627/Model_Card_Claude_3.pdf), 2024.
- Omri Avrahami, Dani Lischinski, and Ohad Fried. Blended Diffusion for Text-driven Editing of Natural Images. In *IEEE Conf. Comput. Vis. Pattern Recog.*, pp. 18208–18218, 2022.
- Jinze Bai, Shuai Bai, Yunfei Chu, Zeyu Cui, Kai Dang, Xiaodong Deng, Yang Fan, Wenbin Ge, Yu Han, Fei Huang, Binyuan Hui, Luo Ji, Mei Li, Junyang Lin, Runji Lin, Dayiheng Liu, Gao Liu, Chengqiang Lu, Keming Lu, et al. Qwen Technical Report. *arXiv preprint arXiv:2309.16609*, 2023.
- Rumeysa Bodur, Erhan Gundogdu, Binod Bhattarai, Tae-Kyun Kim, Michael Donoser, and Loris Bazzani. iEdit: Localised Text-guided Image Editing with Weak Supervision. In *IEEE Conf. Comput. Vis. Pattern Recog.*, pp. 7426–7435, 2024.
- Tim Brooks, Aleksander Holynski, and Alexei A. Efros. InstructPix2Pix: Learning To Follow Image Editing Instructions. In *IEEE Conf. Comput. Vis. Pattern Recog.*, pp. 18392–18402, 2023.
- Tom B. Brown, Benjamin Mann, Nick Ryder, Melanie Subbiah, Jared Kaplan, Prafulla Dhariwal, Arvind Neelakantan, Pranav Shyam, Girish Sastry, et al. Language Models are Few-Shot Learners. *arXiv preprint arXiv:2005.14165*, 2020.
- John Canny. A Computational Approach to Edge Detection. *IEEE Trans. Pattern Anal. Mach. Intell.*, pp. 679–698, 1986.
- Zhe Cao, Gines Hidalgo, Tomas Simon, Shih-En Wei, and Yaser Sheikh. OpenPose: Realtime Multi-Person 2D Pose Estimation Using Part Affinity Fields. *IEEE Trans. Pattern Anal. Mach. Intell.*, 43(1):172–186, 2021. ISSN 0162-8828, 2160-9292, 1939-3539.
- Caroline Chan, Frédo Durand, and Phillip Isola. Learning To Generate Line Drawings That Convey Geometry and Semantics. In *IEEE Conf. Comput. Vis. Pattern Recog.*, pp. 7915–7925, 2022.
- Junsong Chen, Jincheng Yu, Chongjian Ge, Lewei Yao, Enze Xie, Yue Wu, Zhongdao Wang, James Kwok, Ping Luo, Huchuan Lu, and Zhenguo Li. PixArt- $\alpha$ : Fast Training of Diffusion Transformer for Photorealistic Text-to-Image Synthesis. *arXiv preprint arXiv:2310.00426*, 2023a.
- Xi Chen, Lianghua Huang, Yu Liu, Yujun Shen, Deli Zhao, and Hengshuang Zhao. AnyDoor: Zero-shot Object-level Image Customization. *arXiv preprint arXiv:2307.09481*, 2023b.

- Zhe Chen, Jiannan Wu, Wenhai Wang, Weijie Su, Guo Chen, Sen Xing, Muyan Zhong, Qinglong Zhang, Xizhou Zhu, Lewei Lu, Bin Li, Ping Luo, Tong Lu, Yu Qiao, and Jifeng Dai. InternVL: Scaling up Vision Foundation Models and Aligning for Generic Visual-Linguistic Tasks. In *IEEE Conf. Comput. Vis. Pattern Recog.*, pp. 24185–24198, 2024.
- Alibaba Cloud. Tongyi Wanxiang, <https://tongyi.aliyun.com/wanxiang>, 2023.
- Jiankang Deng, Jia Guo, Niannan Xue, and Stefanos Zafeiriou. ArcFace: Additive Angular Margin Loss for Deep Face Recognition. In *IEEE Conf. Comput. Vis. Pattern Recog.*, pp. 4690–4699, 2019a.
- Jiankang Deng, Jia Guo, Debing Zhang, Yafeng Deng, Xiangju Lu, and Song Shi. Lightweight Face Recognition Challenge. In *Int. Conf. Comput. Vis.*, pp. 0–0, 2019b.
- Yuning Du, Chenxia Li, Ruoyu Guo, Xiaoting Yin, Weiwei Liu, Jun Zhou, Yifan Bai, Zilin Yu, Yehua Yang, Qingqing Dang, and Haoshuang Wang. PP-OCR: A Practical Ultra Lightweight OCR System. *arXiv preprint arXiv:2009.09941*, 2020.
- Abhimanyu Dubey, Abhinav Jauhri, Abhinav Pandey, Abhishek Kadian, Ahmad Al-Dahle, Aiesha Letman, Akhil Mathur, Alan Schelten, Amy Yang, Angela Fan, Anirudh Goyal, et al. The Llama 3 Herd of Models. *arXiv preprint arXiv:2407.21783*, 2024.
- Patrick Esser, Sumith Kulal, Andreas Blattmann, Rahim Entezari, Jonas Müller, Harry Saini, Yam Levi, Dominik Lorenz, Axel Sauer, Frederic Boesel, Dustin Podell, Tim Dockhorn, Zion English, Kyle Lacey, Alex Goodwin, Yannik Marek, and Robin Rombach. Scaling Rectified Flow Transformers for High-Resolution Image Synthesis. In *Int. Conf. Mach. Learn.*, 2024.
- FLUX. FLUX, <https://blackforestlabs.ai/>, 2024.
- Yuying Ge, Sijie Zhao, Chen Li, Yixiao Ge, and Ying Shan. SEED-Data-Edit Technical Report: A Hybrid Dataset for Instructional Image Editing. *arXiv preprint arXiv:2405.04007*, 2024a.
- Yuying Ge, Sijie Zhao, Jinguo Zhu, Yixiao Ge, Kun Yi, Lin Song, Chen Li, Xiaohan Ding, and Ying Shan. SEED-X: Multimodal Models with Unified Multi-granularity Comprehension and Generation. *arXiv preprint arXiv:2404.14396*, 2024b.
- Zigang Geng, Binxin Yang, Tiankai Hang, Chen Li, Shuyang Gu, Ting Zhang, Jianmin Bao, Zheng Zhang, Houqiang Li, Han Hu, Dong Chen, and Baining Guo. InstructDiffusion: A Generalist Modeling Interface for Vision Tasks. In *IEEE Conf. Comput. Vis. Pattern Recog.*, pp. 12709–12720, 2024.
- Zhen Han, Chaojie Mao, Zeyinzi Jiang, Yulin Pan, and Jingfeng Zhang. StyleBooth: Image Style Editing with Multimodal Instruction. *arXiv preprint arXiv:2404.12154*, 2024.
- Edward J. Hu, Yelong Shen, Phillip Wallis, Zeyuan Allen-Zhu, Yuanzhi Li, Shean Wang, Lu Wang, and Weizhu Chen. LoRA: Low-Rank Adaptation of Large Language Models. In *Int. Conf. Learn. Represent.*, 2022.
- Jiehui Huang, Xiao Dong, Wenhui Song, Hanhui Li, Jun Zhou, Yuhao Cheng, Shutao Liao, Long Chen, Yiqiang Yan, Shengcai Liao, and Xiaodan Liang. ConsistentID: Portrait Generation with Multimodal Fine-Grained Identity Preserving. *arXiv preprint arXiv:2404.16771*, 2024a.
- Lianghua Huang, Di Chen, Yu Liu, Yujun Shen, Deli Zhao, and Jingren Zhou. Composer: Creative and Controllable Image Synthesis with Composable Conditions. In *Int. Conf. Mach. Learn.*, 2023.
- Yuzhou Huang, Liangbin Xie, Xintao Wang, Ziyang Yuan, Xiaodong Cun, Yixiao Ge, Jiantao Zhou, Chao Dong, Rui Huang, Ruimao Zhang, and Ying Shan. SmartEdit: Exploring Complex Instruction-based Image Editing with Multimodal Large Language Models. In *IEEE Conf. Comput. Vis. Pattern Recog.*, pp. 8362–8371, 2024b.
- Tao Jiang, Peng Lu, Li Zhang, Ningsheng Ma, Rui Han, Chengqi Lyu, Yining Li, and Kai Chen. RTMPose: Real-Time Multi-Person Pose Estimation based on MMPose. *arXiv preprint arXiv:2303.07399*, 2023.

- Zeyinzi Jiang, Chaojie Mao, Yulin Pan, Zhen Han, and Jingfeng Zhang. SCEdit: Efficient and Controllable Image Diffusion Generation via Skip Connection Editing. In *IEEE Conf. Comput. Vis. Pattern Recog.*, pp. 8995–9004, 2024.
- Diederik P. Kingma and Max Welling. Auto-Encoding Variational Bayes. In *Int. Conf. Learn. Represent.*, 2014.
- Alexander Kirillov, Eric Mintun, Nikhila Ravi, Hanzi Mao, Chloe Rolland, Laura Gustafson, Tete Xiao, Spencer Whitehead, Alexander C. Berg, Wan-Yen Lo, Piotr Dollár, and Ross Girshick. Segment Anything. In *Int. Conf. Comput. Vis.*, pp. 4015–4026, 2023.
- KOLORS. KOLORS, <https://github.com/Kwai-Kolors/Kolors>, 2024.
- Pengzhi Li, Qinxuan Huang, Yikang Ding, and Zhiheng Li. LayerDiffusion: Layered Controlled Image Editing with Diffusion Models. *arXiv preprint arXiv:2305.18676*, 2023.
- Zhimin Li, Jianwei Zhang, Qin Lin, Jiangfeng Xiong, Yanxin Long, Xinchu Deng, Yingfang Zhang, Xingchao Liu, Minbin Huang, Zedong Xiao, et al. Hunyuan-DiT: A Powerful Multi-Resolution Diffusion Transformer with Fine-Grained Chinese Understanding. *arXiv preprint arXiv:2405.08748*, 2024.
- Tsung-Yi Lin, Michael Maire, Serge Belongie, James Hays, Pietro Perona, Deva Ramanan, Piotr Dollár, and C Lawrence Zitnick. Microsoft COCO: Common objects in context. In *Eur. Conf. Comput. Vis.*, pp. 740–755, 2014.
- Shilong Liu, Zhaoyang Zeng, Tianhe Ren, Feng Li, Hao Zhang, Jie Yang, Chunyuan Li, Jianwei Yang, Hang Su, Jun Zhu, and Lei Zhang. Grounding DINO: Marrying DINO with Grounded Pre-Training for Open-Set Object Detection. *arXiv preprint arXiv:2303.05499*, 2023a.
- Yang Liu, Cheng Yu, Lei Shang, Yongyi He, Ziheng Wu, Xingjun Wang, Chao Xu, Haoyu Xie, Weida Wang, Yuze Zhao, Lin Zhu, Chen Cheng, Weitao Chen, Yuan Yao, Wenmeng Zhou, Jiaqi Xu, Qiang Wang, Yingda Chen, Xuansong Xie, and Baigui Sun. FaceChain: A Playground for Human-centric Artificial Intelligence Generated Content. *arXiv preprint arXiv:2308.14256*, 2023b.
- Ilya Loshchilov and Frank Hutter. Decoupled Weight Decay Regularization. In *Int. Conf. Learn. Represent.*, 2018.
- Chenlin Meng, Yutong He, Yang Song, Jiaming Song, Jiajun Wu, Jun-Yan Zhu, and Stefano Ermon. SDEdit: Guided Image Synthesis and Editing with Stochastic Differential Equations. In *Int. Conf. Learn. Represent.*, 2021.
- Midjourney. Midjourney, <https://www.midjourney.com>, 2023.
- Ron Mokady, Amir Hertz, Kfir Aberman, Yael Pritch, and Daniel Cohen-Or. Null-text Inversion for Editing Real Images using Guided Diffusion Models. In *IEEE Conf. Comput. Vis. Pattern Recog.*, pp. 6038–6047, 2022.
- Chong Mou, Xintao Wang, Liangbin Xie, Yanze Wu, Jian Zhang, Zhongang Qi, Ying Shan, and Xiaohu Qie. T2I-Adapter: Learning Adapters to Dig out More Controllable Ability for Text-to-Image Diffusion Models. *arXiv preprint arXiv:2302.08453*, 2023.
- Alex Nichol, Prafulla Dhariwal, Aditya Ramesh, Pranav Shyam, Pamela Mishkin, Bob McGrew, Ilya Sutskever, and Mark Chen. GLIDE: Towards Photorealistic Image Generation and Editing with Text-Guided Diffusion Models. *arXiv preprint arXiv:2112.10741*, 2022.
- OpenAI. DALL-E 2, <https://openai.com/dall-e-2>, 2022.
- OpenAI. DALL-E 3, <https://openai.com/dall-e-3>, 2023a.
- OpenAI. GPT-4 Technical Report. *arXiv preprint arXiv:2303.08774*, 2023b.
- OpenAI. Hello GPT-4o, <https://openai.com/index/hello-gpt-4o/>, 2024.

- OpenImage. OpenImage, <https://storage.googleapis.com/openimages/web/index.html>, 2023.
- Long Ouyang, Jeffrey Wu, Xu Jiang, Diogo Almeida, Carroll Wainwright, Pamela Mishkin, Chong Zhang, Sandhini Agarwal, Katarina Slama, et al. Training language models to follow instructions with human feedback. In *Adv. Neural Inform. Process. Syst.*, pp. 27730–27744, 2022.
- Yulin Pan, Chaojie Mao, Zeyinzi Jiang, Zhen Han, and Jingfeng Zhang. Locate, Assign, Refine: Taming Customized Image Inpainting with Text-Subject Guidance. *arXiv preprint arXiv:2403.19534*, 2024.
- William Peebles and Saining Xie. Scalable Diffusion Models with Transformers. In *Int. Conf. Comput. Vis.*, pp. 4195–4305, 2023.
- Can Qin, Shu Zhang, Ning Yu, Yihao Feng, Xinyi Yang, Yingbo Zhou, Huan Wang, Juan Carlos Niebles, Caiming Xiong, Silvio Savarese, Stefano Ermon, Yun Fu, and Ran Xu. UniControl: A Unified Diffusion Model for Controllable Visual Generation In the Wild. *arXiv preprint arXiv:2305.11147*, 2023.
- Alec Radford, Jong Wook Kim, Chris Hallacy, Aditya Ramesh, Gabriel Goh, Sandhini Agarwal, Girish Sastry, Amanda Askell, Pamela Mishkin, Jack Clark, Gretchen Krueger, and Ilya Sutskever. Learning Transferable Visual Models From Natural Language Supervision. *arXiv preprint arXiv:2103.00020*, 2021.
- Colin Raffel, Noam Shazeer, Adam Roberts, Katherine Lee, Sharan Narang, Michael Matena, Yanqi Zhou, Wei Li, and Peter J. Liu. Exploring the Limits of Transfer Learning with a Unified Text-to-Text Transformer. *J. Mach. Learn. Res.*, pp. 1–67, 2020.
- René Ranftl, Katrin Lasinger, David Hafner, Konrad Schindler, and Vladlen Koltun. Towards Robust Monocular Depth Estimation: Mixing Datasets for Zero-Shot Cross-Dataset Transfer. *IEEE Trans. Pattern Anal. Mach. Intell.*, pp. 1623–1637, 2022.
- Robin Rombach, Andreas Blattmann, Dominik Lorenz, Patrick Esser, and Björn Ommer. High-resolution image synthesis with latent diffusion models. In *IEEE Conf. Comput. Vis. Pattern Recog.*, pp. 10684–10695, 2022.
- Nataniel Ruiz, Yuanzhen Li, Varun Jampani, Yael Pritch, Michael Rubinstein, and Kfir Aberman. DreamBooth: Fine Tuning Text-to-Image Diffusion Models for Subject-Driven Generation. In *IEEE Conf. Comput. Vis. Pattern Recog.*, pp. 22500–22510, 2023.
- Chitwan Saharia, William Chan, Saurabh Saxena, Lala Li, Jay Whang, Emily Denton, Seyed Kamyar Seyed Ghasemipour, Burcu Karagol Ayan, S. Sara Mahdavi, Rapha Gontijo Lopes, Tim Salimans, Jonathan Ho, David J. Fleet, and Mohammad Norouzi. Photorealistic Text-to-Image Diffusion Models with Deep Language Understanding. In *Adv. Neural Inform. Process. Syst.*, 2022.
- Christoph Schuhmann, Romain Beaumont, Richard Vencu, Cade W. Gordon, Ross Wightman, Mehdi Cherti, Theo Coombes, Aarush Katta, Clayton Mullis, Mitchell Wortsman, Patrick Schramowski, Srivatsa R. Kundurthy, Katherine Crowson, Ludwig Schmidt, Robert Kaczmarczyk, and Jenia Jitsev. LAION-5B: An open large-scale dataset for training next generation image-text models. In *Adv. Neural Inform. Process. Syst.*, 2022.
- Shelly Sheynin, Adam Polyak, Uriel Singer, Yuval Kirstain, Amit Zohar, Oron Ashual, Devi Parikh, and Yaniv Taigman. Emu Edit: Precise Image Editing via Recognition and Generation Tasks. In *IEEE Conf. Comput. Vis. Pattern Recog.*, pp. 8871–8879, 2024.
- Yujun Shi, Chuhui Xue, Jun Hao Liew, Jiachun Pan, Hanshu Yan, Wenqing Zhang, Vincent Y. F. Tan, and Song Bai. DragDiffusion: Harnessing Diffusion Models for Interactive Point-based Image Editing. In *IEEE Conf. Comput. Vis. Pattern Recog.*, pp. 8839–8849, 2024.
- Gowthami Somepalli, Anubhav Gupta, Kamal Gupta, Shramay Palta, Micah Goldblum, Jonas Geiping, Abhinav Shrivastava, and Tom Goldstein. Measuring Style Similarity in Diffusion Models. *arXiv preprint arXiv:2404.01292*, 2024.

- StabilityAI. Stable Diffusion XL Model Card, <https://huggingface.co/stabilityai/stable-diffusion-xl-base-1.0>, 2022.
- StabilityAI. CosXL Model Card, <https://huggingface.co/stabilityai/cosxl>, 2024.
- Jianlin Su, Yu Lu, Shengfeng Pan, Ahmed Murtadha, Bo Wen, and Yunfeng Liu. RoFormer: Enhanced Transformer with Rotary Position Embedding. *arXiv preprint arXiv:2104.09864*, 2023.
- Keqiang Sun, Junting Pan, Yuying Ge, Hao Li, Haodong Duan, Xiaoshi Wu, Renrui Zhang, Aojun Zhou, Zipeng Qin, Yi Wang, Jifeng Dai, Yu Qiao, Limin Wang, and Hongsheng Li. JourneyDB: A Benchmark for Generative Image Understanding. In *Adv. Neural Inform. Process. Syst.*, 2023a.
- Ya Sheng Sun, Yifan Yang, Houwen Peng, Yifei Shen, Yuqing Yang, Han Hu, Lili Qiu, and Hideki Koike. ImageBrush: Learning Visual In-Context Instructions for Exemplar-Based Image Manipulation. In *Adv. Neural Inform. Process. Syst.*, 2023b.
- Roman Suvorov, Elizaveta Logacheva, Anton Mashikhin, Anastasia Remizova, Arsenii Ashukha, Aleksei Silvestrov, Naejin Kong, Harshith Goka, Kiwoong Park, and Victor Lempitsky. Resolution-Robust Large Mask Inpainting With Fourier Convolutions. In *IEEE Winter Conf. Appl. Comput. Vis.*, pp. 2149–2159, 2022.
- Yuxiang Tuo, Wangmeng Xiang, Jun-Yan He, Yifeng Geng, and Xuansong Xie. AnyText: Multilingual Visual Text Generation and Editing. In *Int. Conf. Learn. Represent.*, 2023.
- Ashish Vaswani, Noam Shazeer, Niki Parmar, Jakob Uszkoreit, Llion Jones, Aidan N Gomez, Łukasz Kaiser, and Illia Polosukhin. Attention is All you Need. In *Adv. Neural Inform. Process. Syst.*, 2017.
- Haofan Wang, Matteo Spinelli, Qixun Wang, Xu Bai, Zekui Qin, and Anthony Chen. InstantStyle: Free Lunch towards Style-Preserving in Text-to-Image Generation. *arXiv preprint arXiv:2404.02733*, 2024a.
- Qixun Wang, Xu Bai, Haofan Wang, Zekui Qin, and Anthony Chen. InstantID: Zero-shot Identity-Preserving Generation in Seconds. *arXiv preprint arXiv:2401.07519*, 2024b.
- Xintao Wang, Liangbin Xie, Chao Dong, and Ying Shan. Real-ESRGAN: Training Real-World Blind Super-Resolution with Pure Synthetic Data. In *Int. Conf. Comput. Vis.*, pp. 1905–1914, 2021.
- Zhizhong Wang, Lei Zhao, and Wei Xing. StyleDiffusion: Controllable Disentangled Style Transfer via Diffusion Models. In *Int. Conf. Comput. Vis.*, pp. 7677–7689, 2023.
- Shaoan Xie, Zhifei Zhang, Zhe Lin, Tobias Hinz, and Kun Zhang. SmartBrush: Text and Shape Guided Object Inpainting With Diffusion Model. In *IEEE Conf. Comput. Vis. Pattern Recog.*, pp. 22428–22437, 2023.
- Yunyang Xiong, Bala Varadarajan, Lemeng Wu, Xiaoyu Xiang, Fanyi Xiao, Chenchen Zhu, Xiaoliang Dai, Dilin Wang, Fei Sun, Forrest Iandola, Raghuraman Krishnamoorthi, and Vikas Chandra. EfficientSAM: Leveraged Masked Image Pretraining for Efficient Segment Anything. In *IEEE Conf. Comput. Vis. Pattern Recog.*, pp. 16111–16121, 2023.
- Jiacong Xu, Zixiang Xiong, and Shankar P. Bhattacharyya. PIDNet: A Real-time Semantic Segmentation Network Inspired by PID Controllers. In *IEEE Conf. Comput. Vis. Pattern Recog.*, pp. 19529–19539, 2023.
- An Yang, Baosong Yang, Binyuan Hui, Bo Zheng, Bowen Yu, Chang Zhou, Chengpeng Li, Chengyuan Li, Dayiheng Liu, Fei Huang, Guanting Dong, Haoran Wei, Huan Lin, Jialong Tang, et al. Qwen2 Technical Report. *arXiv preprint arXiv:2407.10671*, 2024.
- Yukang Yang, Dongnan Gui, Yuhui Yuan, Weicong Liang, Haisong Ding, Han Hu, and Kai Chen. GlyphControl: Glyph Conditional Control for Visual Text Generation. In *Adv. Neural Inform. Process. Syst.*, 2023.

- Hu Ye, Jun Zhang, Sibao Liu, Xiao Han, and Wei Yang. IP-Adapter: Text Compatible Image Prompt Adapter for Text-to-Image Diffusion Models. *arXiv preprint arXiv:2308.06721*, 2023.
- Xiaohua Zhai, Basil Mustafa, Alexander Kolesnikov, and Lucas Beyer. Sigmoid Loss for Language Image Pre-Training. In *Int. Conf. Comput. Vis.*, pp. 11975–11986, 2023.
- Han Zhang, Weichong Yin, Yewei Fang, Lanxin Li, Boqiang Duan, Zhihua Wu, Yu Sun, Hao Tian, Hua Wu, and Haifeng Wang. ERNIE-ViLG: Unified Generative Pre-training for Bidirectional Vision-Language Generation. *arXiv preprint arXiv:2112.15283*, 2021.
- Hua Zhang, Si Liu, Changqing Zhang, Wenqi Ren, Rui Wang, and Xiaochun Cao. SketchNet: Sketch Classification with Web Images. In *IEEE Conf. Comput. Vis. Pattern Recog.*, pp. 1105–1113, 2016a.
- Kai Zhang, Lingbo Mo, Wenhui Chen, Huan Sun, and Yu Su. MagicBrush: A Manually Annotated Dataset for Instruction-Guided Image Editing. In *Adv. Neural Inform. Process. Syst.*, 2023a.
- Kaipeng Zhang, Zhanpeng Zhang, Zhifeng Li, and Yu Qiao. Joint Face Detection and Alignment Using Multitask Cascaded Convolutional Networks. *IEEE Sign. Process. Letters*, pp. 1499–1503, 2016b.
- Lvmin Zhang, Anyi Rao, and Maneesh Agrawala. Adding Conditional Control to Text-to-Image Diffusion Models. In *Int. Conf. Comput. Vis.*, pp. 3836–3847, 2023b.
- Shu Zhang, Xinyi Yang, Yihao Feng, Can Qin, Chia-Chih Chen, Ning Yu, Zeyuan Chen, Huan Wang, Silvio Savarese, Stefano Ermon, Caiming Xiong, and Ran Xu. HIVE: Harnessing Human Feedback for Instructional Visual Editing. In *IEEE Conf. Comput. Vis. Pattern Recog.*, pp. 9026–9036, 2024.
- Youcai Zhang, Xinyu Huang, Jinyu Ma, Zhaoyang Li, Zhaochuan Luo, Yanchun Xie, Yuzhuo Qin, Tong Luo, Yaqian Li, Shilong Liu, Yandong Guo, and Lei Zhang. Recognize Anything: A Strong Image Tagging Model. *arXiv preprint arXiv:2306.03514*, 2023c.
- Haozhe Zhao, Xiaojian Ma, Liang Chen, Shuzheng Si, Rujie Wu, Kaikai An, Peiyu Yu, Minjia Zhang, Qing Li, and Baobao Chang. UltraEdit: Instruction-based Fine-Grained Image Editing at Scale. *arXiv preprint arXiv:2407.05282v1*, 2024.
- Shihao Zhao, Dongdong Chen, Yen-Chun Chen, Jianmin Bao, Shaozhe Hao, Lu Yuan, and Kwan-Yee K. Wong. Uni-ControlNet: All-in-One Control to Text-to-Image Diffusion Models. In *Adv. Neural Inform. Process. Syst.*, 2023.
- Yiming Zhao and Zhouhui Lian. UDiffText: A Unified Framework for High-quality Text Synthesis in Arbitrary Images via Character-aware Diffusion Models. In *Eur. Conf. Comput. Vis.*, 2024.



## A RELATED WORK

Visual generation, which takes multi-modal conditions (*e.g.*, textual instruction and reference image) as input to generate creative image, has emerged as a popular research trend in recent years. As the basic task, text-guided image generation has undergone a significant development, marked by remarkable advancements in recent years. Many approaches (Nichol et al., 2022; Saharia et al., 2022; OpenAI, 2022; Rombach et al., 2022; StabilityAI, 2022; OpenAI, 2023a; Midjourney, 2023; Cloud, 2023; Zhang et al., 2021; Chen et al., 2023a; Esser et al., 2024; KOLORS, 2024; Li et al., 2024; FLUX, 2024) have been proposed and achieved impressive results in terms of both image quality and semantic fidelity. By incorporating low-level visual features as input, Huang et al. (2023) and Zhang et al. (2023b) pave the way for the initial forms of multi-modal controllable generation. Recently, some approaches (Mou et al., 2023; Zhao et al., 2023; Qin et al., 2023) have tried to use multiple visual features as conditions, facilitating the multi-modal controllable generation. By integrating fine-tuning technologies such as Ruiz et al. (2023); Hu et al. (2022), these approaches have further enabled the customization of diverse controllable generation applications. Another popular trend is image editing technology (Ye et al., 2023; Han et al., 2024; Wang et al., 2024b; Huang et al., 2024a; Wang et al., 2024a; Liu et al., 2023b; Tuo et al., 2023; Chen et al., 2023b; Pan et al., 2024; Wang et al., 2023; Xie et al., 2023; Sun et al., 2023b; Huang et al., 2024b; Bodur et al., 2024; Shi et al., 2024; Li et al., 2023; Meng et al., 2021), which focus on editing input images according to text prompts and preserving some identity such as person, scene, subject, or style. While the above models excel at generating image in one specific task or scenario, they have difficulty in extending to unseen tasks. To address the aforementioned challenges, some methods have been introduced to edit input images by following natural language instructions (Brooks et al., 2023; StabilityAI, 2024; Geng et al., 2024; Sheynin et al., 2024; Zhao et al., 2024; Ge et al., 2024b) which is more flexible to implement various tasks within a single model. However, a key bottleneck for these methods lies in the construction of high-quality instruction-paired datasets with annotated edits, which cause limited generalizability and suboptimal performance. In this paper, we focus on establishing a unified definition for multi-modal generation problems. Based on this definition, we aim to construct higher-quality, annotated data and instruction sets further to develop a unified foundational model for multimodal generation.

## B DATASETS DETAIL

We use an internal dataset of 0.7 billion data pairs to train a foundational model for generation and editing. The supported tasks include **8** basic types consisting of **37** subtasks, as well as a multi-turn and long-context generation task. These tasks use textual instructions along with zero or more reference images for generating or editing image. The data distribution is depicted in Fig. 6a, and the absolute data scale is illustrated in Fig. 6b. In this section, we provide a detailed introduction to the data construction methods for various tasks.

### B.1 TEXT-GUIDED GENERATION

We collect approximately 117 million images and use MLLM model to supplement captions for images, creating pair data for text-to-image tasks. Additionally, this portion of the data serves as an intermediary bridge in various generation and editing tasks, allowing the combination of different task instructions to obtain pairs from original images to target images.

### B.2 LOW-LEVEL VISUAL ANALYSIS

Low-level Visual Analysis tasks involve analyzing and extracting various low-level visual features from a given image, like an edge map or segmentation map. These low-level visual features are typically employed as control signals in the controllable generation. We select 10 commonly used low-level features in the controllable generation, including segmentation map, depth map, human pose, mosaic image, blurry image, gray image, edge map, doodle image, contour image, and scribble image. The visual features extracted at global and local levels are illustrated in Fig. 7 and Fig. 8, respectively.

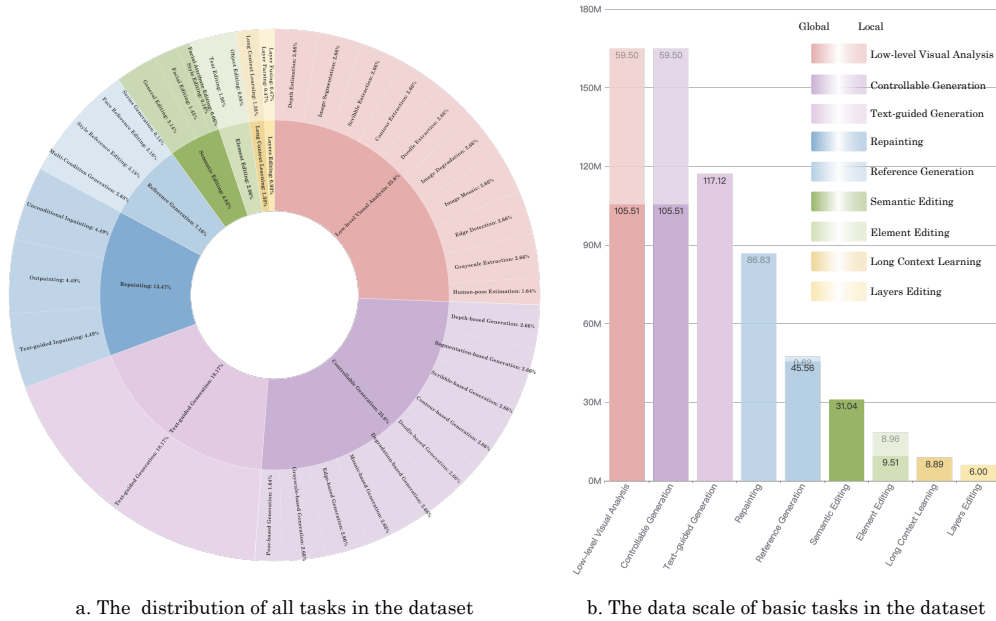


Figure 6: **Statistics on the data scale for various tasks.** We collect 0.7 billion data pairs, which cover 8 basic types including 37 subtasks, multi-turn and long-context generation datasets.

- **Image Segmentation** involves extracting image spatial region information for different targets within an image. This is achieved by selecting and modifying specific areas for operations and editing in downstream tasks. We employ the Efficient SAM (Xiong et al., 2023) tool for marking different target areas within an image.
- **Depth Estimation** indicates the relative distance information of different targets within an image. We use the Midas (Ranftl et al., 2022) algorithm to extract depth information.
- **Human-pose Estimation** is employed for modeling the human body to obtain structured information about body posture. We make use of the RTMPose (Jiang et al., 2023) algorithm to extract information from images containing human figures, and posture information visualization is done using OpenPose’s 17-point (Cao et al., 2021) modeling method.
- **Image Mosaic** pixelates specific areas or the entire image to protect sensitive information.
- **Image Degradation** is used to degrade the quality of an image to simulate the phenomenon of image distortion found in the real world. Following the practice of super-resolution algorithms (Wang et al., 2021), we add random noise to the input images.
- **Image Grayscale** is typically done to facilitate the editing of an image’s original colors downstream. We do this conversion directly using OpenCV’s Grayscale function.
- **Edge Detection** detects the edge information from the original image. We utilize the edge detection method named Canny (Canny, 1986) implemented by OpenCV.
- **Doodle Extraction** is usually used to simulate relatively rough hand-drawn sketches by extracting the outline of objects and ignoring their details. We use the PIDNet (Xu et al., 2023) and SketchNet (Zhang et al., 2016a) to extract this information.
- **Contour Extraction** is about delineating the outline of targets within an image, which simulates the drawing process of the image and is often used for secondary processing of images. We use the contour module from the informative drawing (Chan et al., 2022) for this information extraction.
- **Scribble Extraction** involves retrieving the original line art information to capture the sketch-like form of the image. We utilize the anime-style module from informative drawings (Chan et al., 2022) to extract the relevant information.

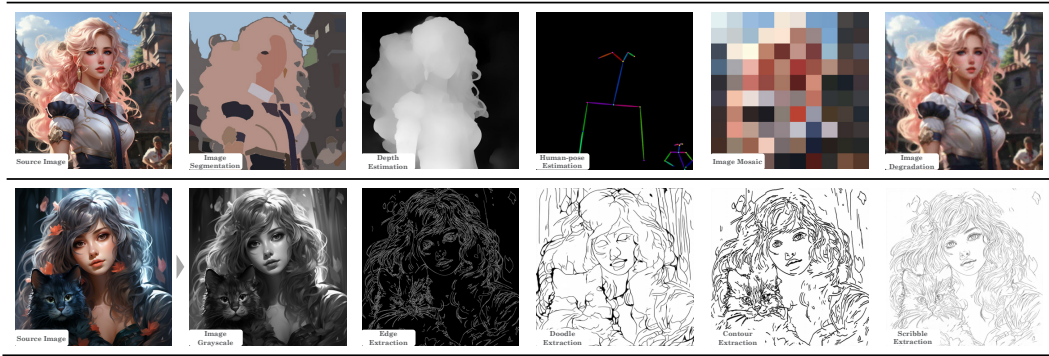


Figure 7: The visualization of low-level visual analysis preprocessing.



Figure 8: The visualization of regional low-level visual analysis preprocessing.

### B.3 CONTROLLABLE GENERATION

In the realm of vision-based generative foundation models, the ability to generate corresponding content using any provided prompts is commonly present. To further control aspects such as spatial layout, structure, or color in the generated images, additional conditional information is often incorporated as inputs to the model. We integrate various controllable condition-to-image tasks within a unified framework to accommodate different visual conditions. The control conditions include the visual features mentioned in the low-level visual analysis section. For training data, we employ pairs constituted by the aforementioned control conditions in Fig. 7 and regional control conditions in Fig. 8 obtained through low-level visual analysis, using the conditional part as inputs to the model to achieve pixel-precise image generation. For text guidance, we construct the instructions based on image captions with our proposed Instruction Captioner.

### B.4 SEMANTIC EDITING

Semantic Editing aims to modify specific semantic attributes of an input image by providing detailed instructions. It involves facial editing, which aims to modify partial attributes of characters while preserving the overall identity, and style transforming, which aims to transform the image style to a specific artist theme guided by instruction while keeping content unchanged. Additionally, any other semantic editing requests that do not fall into these two categories are classified as general editing, *e.g.*, changing the background scene of an image, adjusting a subject’s posture, and modifying the camera view. We discuss the specifics according to the particular tasks.

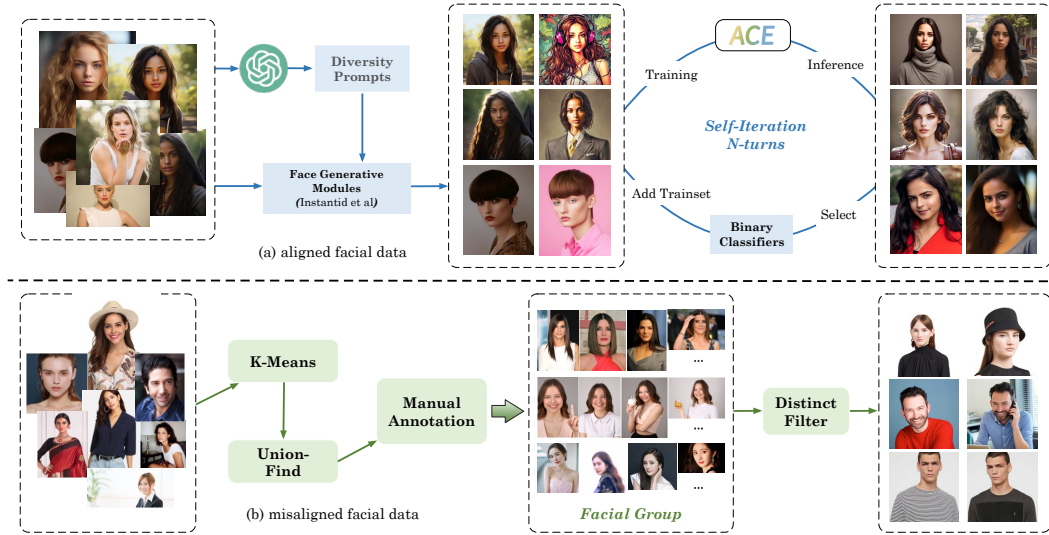


Figure 9: Illustration of facial editing data processing workflow.

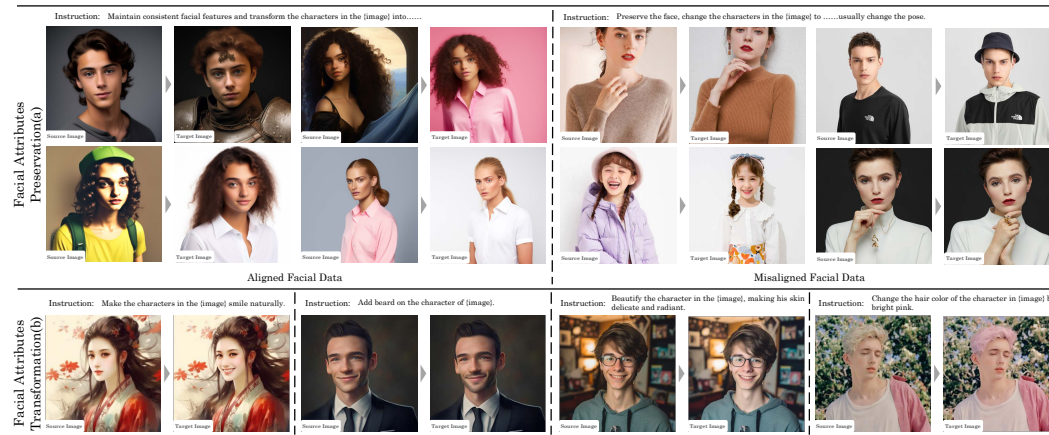


Figure 10: The dataset visualization of facial editing.

#### B.4.1 FACIAL EDITING

Facial Editing encompasses both the transformation and preservation of facial attributes. Specifically, the facial attributes preservation task focuses on editing other elements of the image while maintaining the consistency of complex identity details in facial representations. The facial attributes transformation task is primarily concerned with altering specific attributes of the face without affecting other aspects of the image.

**Facial Attribute Preservation.** The facial attribute preservation dataset is divided into two main parts: aligned and misaligned facial data as shown in Fig. 10a. There are two novel processing workflows as shown in Fig. 9. **(i) Aligned facial data.** We generate pixel-aligned face data using generative models such as InstantID (Wang et al., 2024b) and combine it with GPT models to produce diverse prompts. Subsequently, we train multiple lightweight binary classification models to clean the generated data based on image quality, PPI score, aesthetic scores, and other metrics. Additionally, we extract facial features using ArcFace (Deng et al., 2019a) for similarity calculations, selecting high-matching data pairs with a similarity score exceeding 0.65. Once our model demonstrates the ability to maintain facial integrity, we initiate a self-iterative training process to generate higher quality data, as illustrated in Fig. 9a. **(ii) Misaligned facial data.** We first employ a face detection algorithm (Zhang et al., 2016b) to filter images containing only one face. Subsequently, we utilized facial features to perform K-means clustering, resulting in 10,000 clusters. Within each



Figure 11: The dataset visualization of style editing.

cluster, we conducted a second clustering using the union-find algorithm. Faces with a similarity score greater than 0.8 and less than 0.9 were linked to avoid grouping perfectly identical images. Finally, manual annotation and deduplication were performed on the remaining clusters, yielding the final unaligned facial dataset as shown in Fig. 9b. Based on the general instruction construction process in Sec. 3.2, we design the instructions for facial editing to emphasize that the individuals in the image pairs being annotated are the same person. The instructions must reflect this and focus on the differences in personal details between the two images.

**Facial Attribute Transformation.** We add four fine-grained facial attribute transformation tasks: smiling, beard, makeup, and hair dyeing. We obtained the relevant data in bulk by calling the Aliyun API and trained binary classifiers for each category to filter out data with indistinct changes. As a result, we acquired a total of 1.4 million high-quality pairs of data as shown in Fig. 10b. Equally, we strive to guide the generated captions to closely reflect the facial attributes, thereby enhancing the model’s understanding of the similarities and differences in tasks related to facial attributes.

#### B.4.2 STYLE EDITING

Following the similar image pair construction strategy from StyleBooth (Han et al., 2024), we prepare a larger training data that encompasses over 80 styles and 63000 image pairs. Besides, additional real-world and synthesized style images are collected as style editing target images, and their corresponding “original” images are generated by transforming these collected images to different graphic styles such as cinematic, photography, etc. In this way, we obtain around 70000 input and output image pairs of about 400 high-quality styles. We show samples of the final style editing data in Fig. 11.

We conduct different filter strategies to leverage the data quality: (i) Like StyleBooth, we use CLIP score as the metric to filter out the image pairs which have too minor or too great differences. (ii) To further filter out the faultful synthesized target images that are not particularly aligned with the provided prompt keywords in terms of style, we use CSR (Somepalli et al., 2024) representations and implement style clustering within every style subgroup. Setting a threshold of 0.65, cosine similarities are calculated for union-find clustering. The largest cluster contains images in a similar visual style while other clusters are filtered out.

#### B.4.3 GENERAL EDITING

The objective of general editing is to curate an image that seamlessly harmonizes with both textual and visual prompts for a variety of purposes. It involves two tasks, *i.e.*, caption-guided image generation and instruction-guided image adaption. The former task receives one reference image and one caption as prompts to generate the image, and the latter task intends to adapt the source image by following the given instructions. The training data for these two tasks can be unified into the same format, which consists of a content-related image pair  $(I_{source}, I_{target})$ , and a text prompt indicates how to generate target image. An essential goal of building such a training dataset is to acquire content-related image pairs, one of which serves as the source image and another serves as target image. The overall dataset construction pipeline is depicted in Fig. 12. It includes two branches, *i.e.*, **clustering-based** method, and **synthesis-based** method.



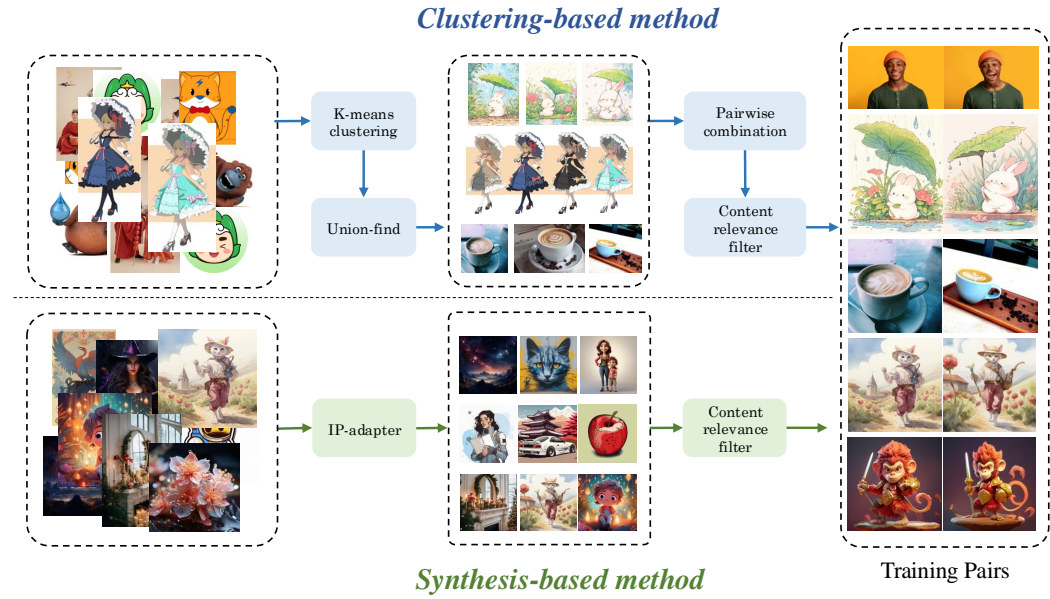


Figure 12: The dataset construction pipeline for general editing task.



Figure 13: **General editing sample pairs generated by our dataset construction pipeline.** Image pairs in the first row are generated by cluster-based method, and those in the second row are generated from synthesis-based method.

**Cluster-based method.** We employ embedding-based clustering on the database to group content-similar images. Union-find technology is employed inside each cluster to achieve more fine-grained image pair aggregation. We then collect all possible pairs from each disjoint set. Additionally, a binary classifier evaluates the content relevance of pairs, and those with low relevance are discarded.

**Synthesis-based method.** We use IP-Adapter technology to synthesize images according to the reference images and text prompts, thus the content-related image pairs can be obtained. To ensure visual content is similar but not the same, we set the image control strength  $\lambda$  to 0.6, and a binary classifier is utilized to filter out content-unrelated pairs. We depict some generated samples in Fig. 13.

For the text prompt of each image pair, we use the MLLM to generate both a caption that describes the visual content of the target image, and an instruction that indicates how to adapt the source image to the target image, as described in Sec. 3.2.

### B.5 ELEMENT EDITING

Element editing focuses on the selective manipulation of specific subjects within an image. This process allows for the addition, deletion, or replacement of a particular subject while ensuring that the other elements within the image remain unchanged. By doing so, the integrity of the overall com-

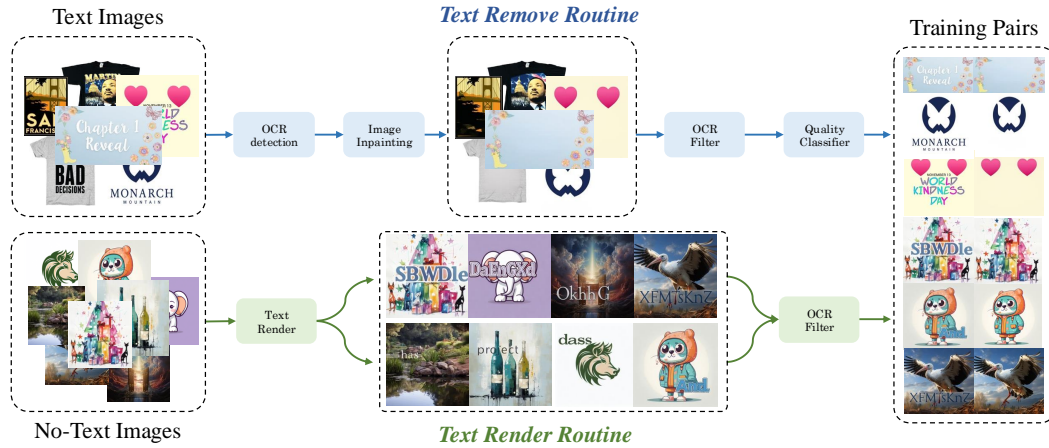


Figure 14: The pipeline of building training data of text editing.

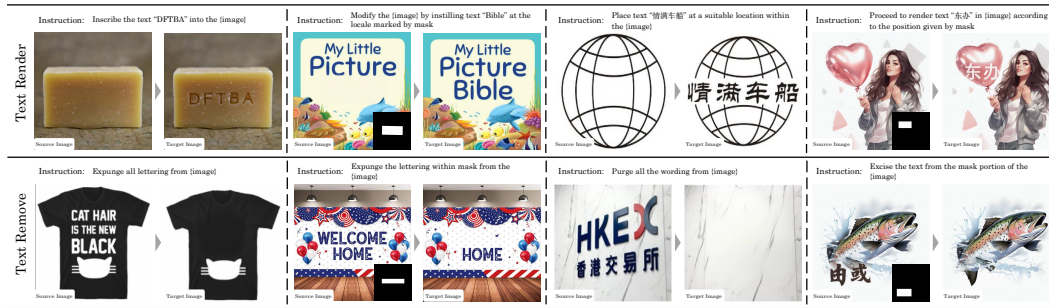


Figure 15: The dataset visualization of multi-lingual text editing.

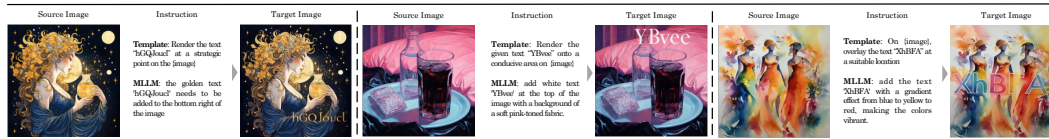


Figure 16: Template-based instructions and MLLM-based instructions on text editing.

position is preserved, allowing users to make precise edits and achieve desired alterations without disrupting the context of the original scene. We focus on two common elements: text and objects.

### B.5.1 TEXT EDITING

Text editing is an important task of element editing. Despite the progress gained in image generation, the capability of text rendering is still far from satisfying. Therefore, text editing is a necessary technology to revise the incorrect or deformed text rendered in image. Text editing involves text removing task, which is to erase text from image while preserving all other visual cues, and text rendering task, which is to render specific text at any location of an image. The goals of these two tasks are exactly the opposite, hence their training data can be shared to each other. For instance, for any image pair  $\{I_a, I_b\}$ , suppose the text removing represents the generation direction from  $I_a$  to  $I_b$ , on the contrary, the generation direction from  $I_b$  to  $I_a$  stands for text rendering. Therefore, the objective of constructing the dataset thus becomes how to obtain a large number of image pairs, where one image contains the specified text and the other does not while keeping the non-text content unchanged.

We propose a two-branch data collection method to address this issue. The overall pipeline shown in Fig. 14 includes two paths: (i) **Text remove path**. For images containing text data, which typi-



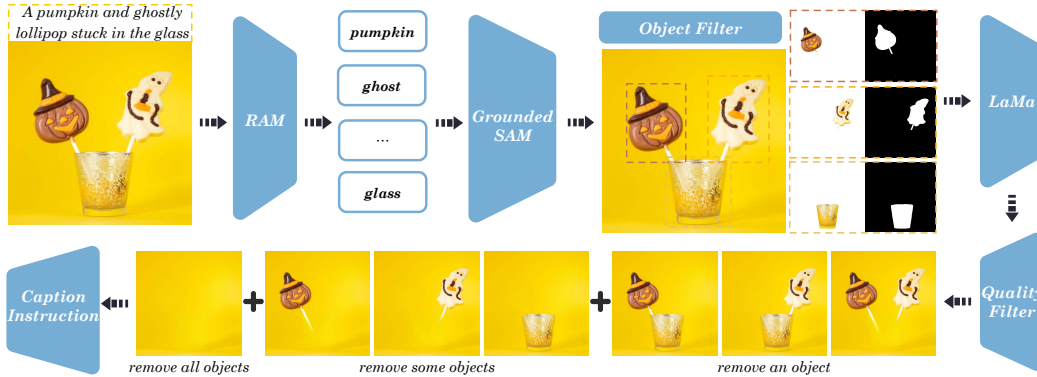


Figure 17: Illustration of data construction pipeline for object editing in element editing.

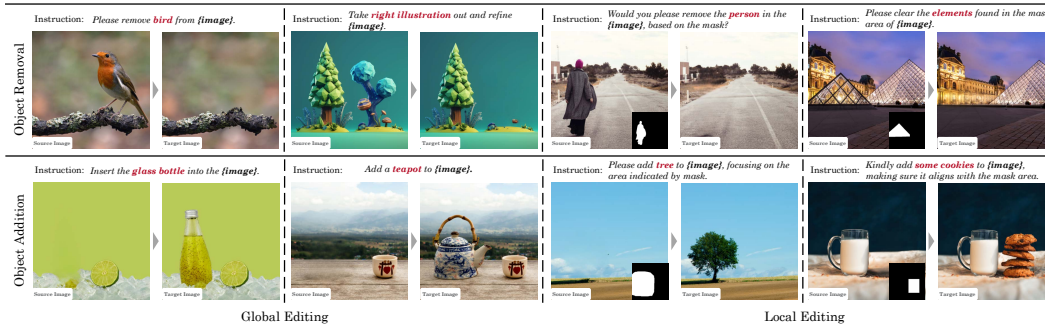


Figure 18: The dataset visualization of object editing in element editing.

cally from publicly available text datasets such as AnyWord3M (Tuo et al., 2023) and LaionGlyph-10M (Yang et al., 2023), we first mask out all text regions. Then, we redraw the masked areas leveraging image inpainting method. To ensure the regenerated image does not contain any textual information, we employ OCR detection leveraging the open-sourcing OCR model (e.g., PP-OCR) (Du et al., 2020) and filter out all images that contain any texts. Finally, we adopt an image quality score predictor which is trained with small amounts of manually annotated data to score all text-removed images and pick high-quality samples according to the score. (ii) **Text render path.** For any image dataset, We first employ OCR detection to ensure input images contain no text. Then random characters are rendered in random locations of these images by utilizing existing text editing methods (e.g., AnyText) (Tuo et al., 2023). We render text using Chinese or English characters to support multi-lingual text rendering capability. We depict some cases in Fig. 15. Finally, we implement OCR detection on the edited image to ensure all characters are rendered correctly. When training, image pairs collected from both two paths are merged to form the total dataset.

We adopt template-based and MLLM-based methods to construct instructions that describe how to render or remove text from the input image. For MLLM-based method, besides the content of characters, we add extra color and position controls by specifying the text color and render position in the textual instruction. Given a text image, we utilize a pre-trained MLLM to describe the color, content, and position information of text in this image, thus a text editing instruction can be easily inferred based on these descriptions. Some cases of template-based and MLLM-based instructions are illustrated in Fig. 16.

### B.5.2 OBJECT EDITING

Object-based image editing is one of the most commonly used techniques for creatively manipulating images. Its primary goal is to either remove or add objects in an image based on text instructions provided by the user, while ensuring a harmonious composition. To obtain training data for this task, we need to construct a pair of data to indicate the presence relationship of objects. Specifically, we

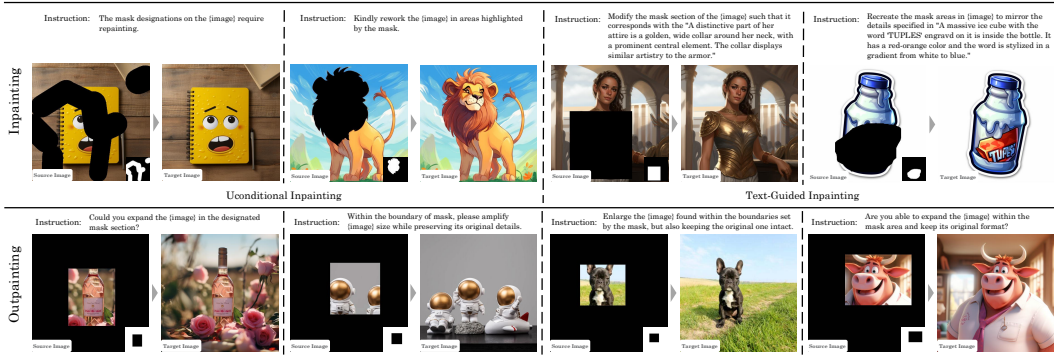


Figure 19: The dataset visualization of Repainting.

focus on images that either contain a specific object or do not, ensuring that all other parts of the images remain as unchanged as possible, except for the area where the object is located.

We can see the entire dataset process from Fig. 17. We first utilize RAM (Zhang et al., 2023c) for open-label tagging, obtaining semantic labels for different subjects in the image, and then applying Grounded-SAM (Liu et al., 2023a; Kirillov et al., 2023) to segment the input semantics. Next, we perform a preliminary screening of objects based on filtering criteria including the area of the masks and bounding boxes, as well as their effective ratios, removing any unreasonable subjects. We then use the LaMa (Suvorov et al., 2022) method, combining the original image with the subject mask area for inpainting. This operation effectively removes local objects without significantly affecting other areas. Finally, we employ a pre-trained binary classification model to determine whether the inpainted image meets expectations, filtering out artifacts introduced by the inpainting algorithm. In terms of instruction formulation, we employ a template format that incorporates the {object\_name} tag, while also utilizing a common instruction based on image pairs.

Through the data construction pipeline, we can obtain the original image, the image with the object removed, the object mask, and the corresponding text instructions. This way, we can implement a forward pipeline for object removal and a reverse pipeline for object addition, while ensuring the integrity of the image and the accuracy of the text instructions, as in Fig. 18.

## B.6 REPAINTING

The repainting task can be defined as the process of reconstructing missing image information within specified masked regions. Depending on the location of the masked area and input conditions, this task can be categorized into three distinct types: unconditional inpainting, text-guided inpainting, and outpainting. Some examples of training data are shown in Fig. 19.

### B.6.1 UNCONDITIONAL INPAINTING

Unconditional image inpainting typically utilizes methods such as low-level textual information and Fourier Convolutions, combined with contextual information from the known areas of the image, to reconstruct the missing portions. This process usually requires an input consisting of an image to be inpainted and a mask indicating the regions that need to be filled, leading to an output image where the missing areas are completed. The task demands that the original information is preserved and that there is a high-quality seamless integration between the original and the filled-in areas. By employing LaMa’s (Suvorov et al., 2022) mask generation strategy, we randomly apply bbox or irregular-shaped masks to the images and vary the degree of this operation to enable the model to handle different types of missing regions as effectively as possible.

### B.6.2 TEXT-GUIDED INPAINTING

Text-guided inpainting primarily aims to fill and restore missing parts of an image by utilizing text descriptions to guide the process. Unlike traditional unconditional inpainting, this method integrates textual information to guide the model, resulting in images that better meet the user’s specific

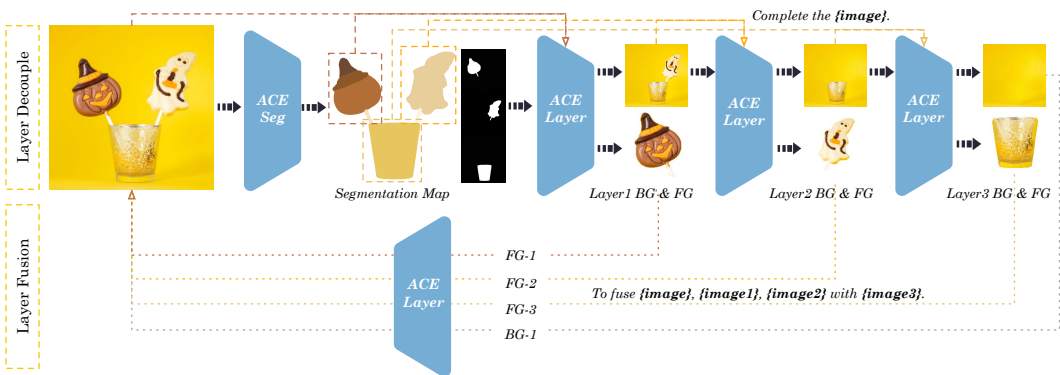


Figure 20: Illustration of inference pipeline layer decouple and layer fusion in layer editing.

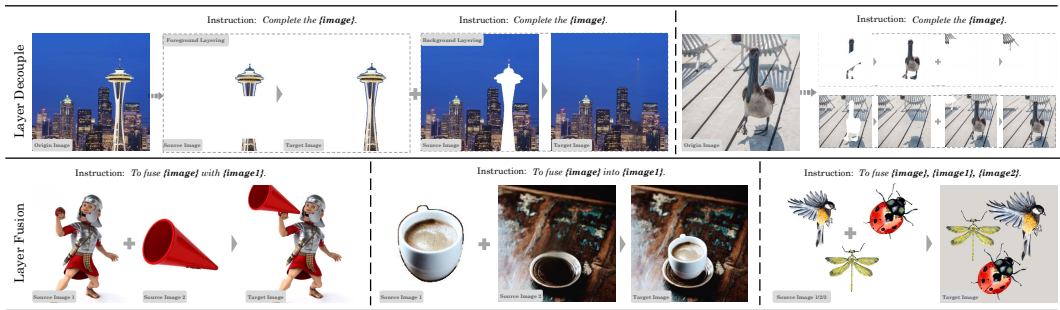


Figure 21: Sample data for training layer decouple and layer fusion in layer editing.

requirements. In constructing this dataset, we not only employ random masks paired with corresponding textual descriptions of the original images but also refine the process to focus on local regions. First, we obtain multiple object masks from the image, and then extract detailed textual descriptions for each object. Finally, we create triplets consisting of the original image, the local object mask, and the local object caption. This approach enables the generation of richer and more controllable details within local areas.

B.6.3 OUTPAINTING

The outpainting task involves intelligently generating and completing the edge regions of an existing image so that the extended new image appears natural and continuous visually. The major challenge of this task is producing images that are rich in detail, diverse in content, and exhibit a certain level of associative ability. In terms of data processing, we employed commonly used techniques, applying random masks to the areas and directions that need to be expanded, in order to adapt to different scenarios of image completion.

B.7 LAYER EDITING

Hierarchical layer editing operations on images involve two aspects: (i) **Layer decouple**: enables the separation of the main subject within a single image, resulting in a complete subject and a reconstructed background. The subject must be restored to its complete form, mitigating any gaps caused by occlusion or other reasons present in the original image. Meanwhile, the background is filled in for the blank areas left after the subject’s separation, achieving a fully deconstructed fore/background. (ii) **Layer fusion**: allows for the incorporation of distinct independent subjects into a target image, facilitating high-quality image integration. The inference pipeline can be seen in Fig. 20.

For the data construction, we follow the data workflow from the object editing task, focusing on slightly larger subjects and data containing multiple subjects within a single image. This approach



Figure 22: The dataset visualization of multi-reference.

creates compositions that allow for a lossless splitting of a single original image into multiple sub-images, and conversely establishes a correspondence for combining several images into one. Specifically, as shown in Fig. 21, in layer decouple stage, we follow the instructions to transition from the original image to either a singular subject or a singular background. During training, the non-subject areas of the subject image and the incomplete portions of the background are filled with white color. Additionally, to simulate the scenario of subjects obscured in the image, we perform random masking on the extracted subject images. The output targets are the complete subject or background. In layer fusion stage, we employ a multi-reference image strategy, taking single or multiple subjects along with the background as inputs to guide the generation of the target image. Similarly, different subjects are supplemented with white color and placed on a randomly sized white canvas, with the training goal being to generate a harmonious and complete composite image.

## B.8 REFERENCE GENERATION

Ordinary image generation and editing tasks require no more than one input image. Under certain circumstances, image generation needs multiple image inputs, such as multiple conditions in con-



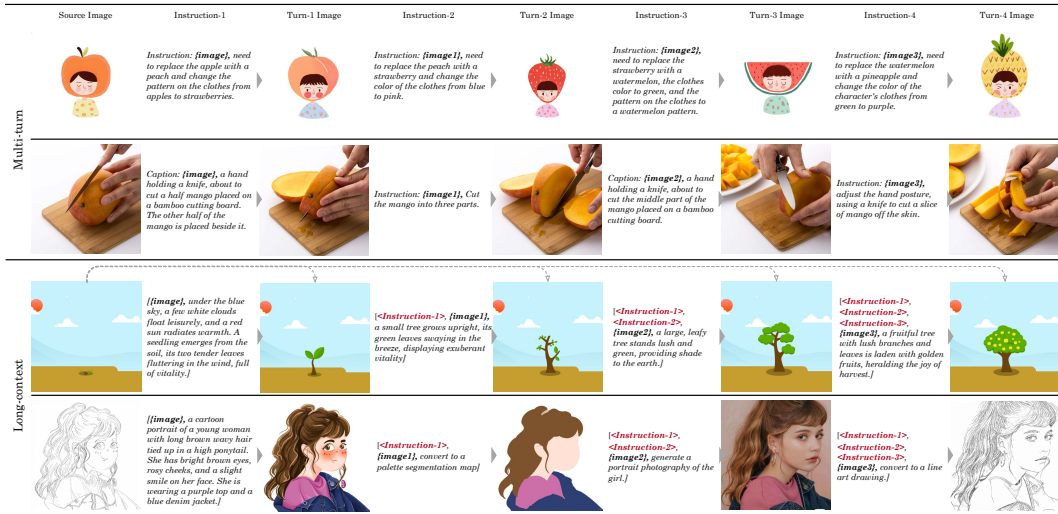


Figure 23: Sample data for training multi-turn and long-context generation task.

trollable generation, and a group of character design images for ID preservation. The same is true for editing tasks, one or more additional exemplar images are necessary to specify the expected visual elements in the editing area. For example, a reference image can be interpreted as the target image style appearance, face identity, etc. Therefore, we prepare training data for multi-reference generation and reference-guided editing. Examples of training data are shown in Fig. 22.

B.8.1 MULTI-REFERENCE GENERATION

**Multi-condition generation.** In controllable generation, overlaying different types of conditions is usually necessary to control the different visual aspects of generated images. Similar to the process in appendix B.3, canny edge maps, depth maps, color maps, grayscale images, contours, scribbles, doodles, and pose keypoints are included for multi-condition generation. To make it possible to composite objects in different conditions, we use object segmentation to assign each area with a different condition.

**Series Generation.** It has been widely studied how to generate images about one consistent visual element, like the portrait of a specific figure, pictures with the same styles, etc. Usually, tuning a themed tuner (e.g., LoRA) (Hu et al., 2022) with few images is the primary option. However, we are aiming to teach our model to understand and follow the rules lying behind image series. We collect image groups through image clustering. During the training phase, we randomly sample one image in the cluster as a target and 3 to 8 images as input images.

B.8.2 REFERENCE-GUIDED EDITING

Style and face are two typical editing tasks benefiting from additional reference image inputs, providing supplementary visual information of the target images.

**Style reference editing.** To construct the training data, we extend the data of style editing (appendix B.4.2) by assigning an additional style reference image for each edit-target image pair. Reference images are randomly selected from other styled images within the same style category.

**Face reference editing.** We use image pairs of misaligned facial data (appendix B.4.1) for face reference editing. We pick one of the two images as reference image while another as target image. Therefore, the target and reference image are the same person but slightly different. The edit image is derived from target image by erasing the face area to avoid any spoilers.

B.9 MULTI-TURN AND LONG-CONTEXT GENERATION

Multi-turn editing refers to the process of obtaining the final image from an input image through multiple independent instruction-based editing, which poses significant challenges in both the model’s

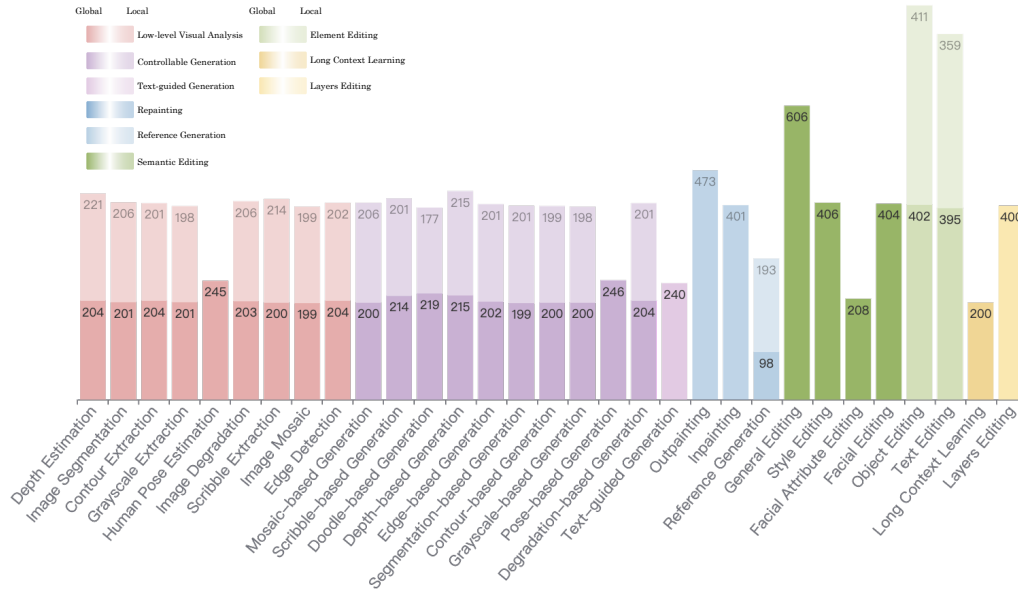


Figure 24: **The overview of benchmark distribution.** “Global” and “Local” refer to editing or generating based on the entire image, and editing or generating based on specific local areas of the image, respectively.

Table 3: The comparison between ACE benchmark and existing benchmarks.

Benchmark	Real Image?	Generated Image?	Multi-turn?	Regional?	Tasks	Data Scale
MagicBrush	Y	N	Y	Y	-	1588
Emu Edit	Y	N	N	N	8	3589
ACE	Y	Y	Y	Y	31	12000

precise understanding of instructions and the control over image quality in every round. Further, the long-context generation process aims to leverage the contextual information provided in each round of interactions to construct a long sequence, thereby generating images that align with the intended directives. The generated images reference multiple images and their corresponding instruction information from previous interactions, capturing the user’s genuine intent within the interaction framework, and allowing for more precise image editing.

The data construction consists of two parts: (i) Homogenous content-based condition unit: this involves employing a pair data collection strategy to obtain various clusters from a large-scale database, as shown in Sec. 3.1, where each cluster contains images paired with their respective captions and instruction generated in pairs. During training, we select one image from any chosen cluster as the starting point and build a multiple rounds data chain using its caption or instruction, predicting the final image as the endpoint of the chain. (ii) Task-based condition unit: we treat all the previously mentioned single-image tasks as individual turns within the task and randomly sample them to form a complete multiple precursor unit that guides the final image generation.

### C BENCHMARK DETAILS

Previous methods have proposed benchmarks to evaluate model performance for image editing, with notable examples including MagicBrush (Zhang et al., 2023a) and Emu Edit (Sheynin et al., 2024). MagicBrush has 1,588 samples, which includes 1,053 single-turn and 535 multi-turn instances, and primarily comes from MS-COCO (Lin et al., 2014). Emu Edit first defines 8 different categories of potential image editing operations and constructs the instructions by human annotators. The main issues with the above methods are insufficient coverage of tasks and generally poor data quality.

Table 4: The multi-stage training details for ACE.

Stage	Model Capacity	Train Data Scale	Visual Sequence Length	Max Image Number	Training Steps	Batch Size
Instruction Align	0.6B	0.7 Billion	1024	1	900K	800
Instruction Align	0.6B	0.7 Billion	1024	9	100K	400
Aesthetic Improvement	0.6B	50 million	1024	9	500K	400
Aesthetic Improvement	0.6B	50 million	4096	9	100K	960

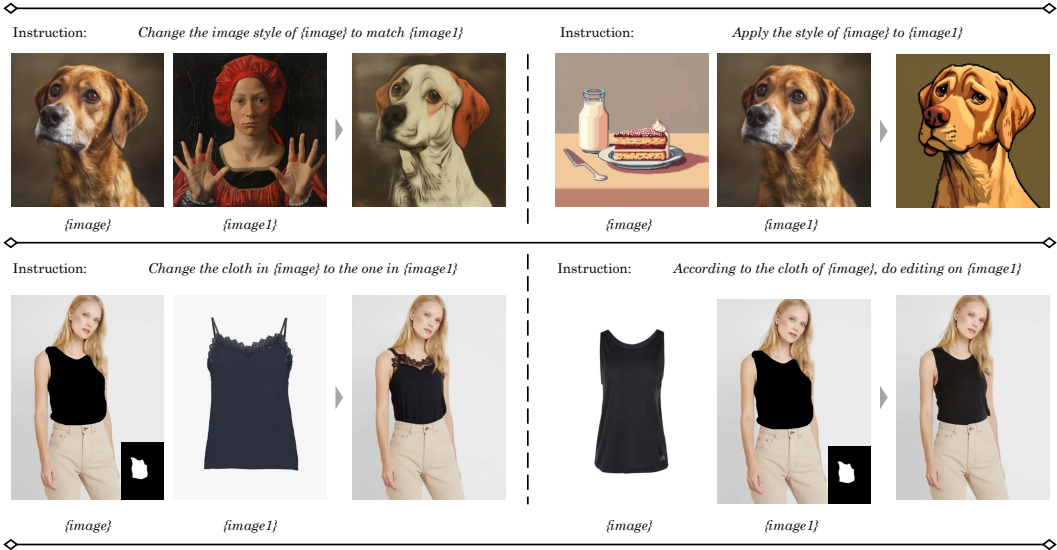


Figure 25: **The effectiveness of Image Indicator Embeddings.** Model follows the image indicators in instructions to distinguish the source and reference images.

ACE builds a benchmark comprising 12,000 samples, covering more than 31 tasks while accommodating 5900 real images and 6100 generated images. In addition, ACE benchmark supports both regional editing and multi-turn editing tasks. The specific statistics are shown in the Fig. 24, and the comparison with other benchmarks is presented in the Tab. 3.

## D IMPLEMENTATION DETAILS

We employ the T5 language model as the text encoder and DiT-XL/2 (Peebles & Xie, 2023) as the base network architecture. The model capacity is nearly 0.6B and the parameters are partly initialized by PixArt- $\alpha$  (Chen et al., 2023a). The maximum length of the text token sequence is set to 120. We freeze VAE and T5 modules, utilizing AdamW (Loshchilov & Hutter, 2018) optimizer to train the DiT module with a weight decay of  $5e-4$  and a learning rate of  $2e-5$ . All experiments are conducted in A800.

A multi-stage training strategy is employed to progressively enhance the aesthetic quality and increase the generalizability of model. The training details are presented in Tab. 4. First, we train the instruction-following capability on single-image tasks using 0.7 billion data points, with the number of single image tokens limited to 1024. Next, we expand the tasks to include multiple-image scenarios. After learning the instruction alignment, we utilize high-aesthetic data to enhance the model’s aesthetics and extend the max image token number to 4096 for generating higher-resolution image.

## E MORE EXPERIMENTS

**Design of Image Indicator Embeddings.** We test the effectiveness of Image Indicator Embeddings by adjusting the order of input images. As we can see in Fig. 25, the model always understands which image is the source image and which is the reference following the image indicators in the



Table 5: Results on Emu Edit benchmark. ACE shows comparable performance to its baselines.

Method	CLIPdir↑	CLIPout↑	L1↓	CLIPimg↑	DINO↑
InstructPix2Pix (Brooks et al., 2023)	0.0739	0.2681	0.1240	0.8508	0.7647
MagicBrush (Zhang et al., 2023a)	0.0831	0.2701	0.0995	0.8664	0.7927
Emu Edit (Sheynin et al., 2024)	<b>0.1073</b>	<b>0.2791</b>	0.0893	0.8743	0.8398
UltraEdit (Zhao et al., 2024)	0.0888	<u>0.2783</u>	<b>0.0532</b>	<u>0.8814</u>	<u>0.8524</u>
CosXL (StabilityAI, 2024)	<u>0.0901</u>	0.2775	0.0940	0.8686	0.8340
<b>ACE (Ours)</b>	0.0855	0.2746	<u>0.0761</u>	<b>0.8952</b>	<b>0.8620</b>

Table 6: Quantitative results for Facial Editing tasks on ACE benchmark. † indicates that InstantID requires an additional landmark as a condition, while other methods do not.

Method	Face Similarity	Effective Score
InstantID† Wang et al. (2024b)	84.08	0.96
CosXL StabilityAI (2024)	66.49	0.37
UltraEdit Zhao et al. (2024)	62.91	0.16
IP-Adapter Ye et al. (2023)	<u>66.51</u>	0.31
FaceChain Liu et al. (2023b)	65.46	<u>0.42</u>
<b>ACE (Ours)</b>	<b>70.07</b>	<b>0.67</b>

Table 7: Quantitative results for Local Text Render tasks on ACE benchmark.

Method	Edit Distance	Sentence Accuracy
UDiffText (Zhao & Lian, 2024)	<u>0.6827</u>	<u>0.4110</u>
AnyText (Tuo et al., 2023)	0.6035	0.3313
<b>ACE (Ours)</b>	<b>0.8211</b>	<b>0.5767</b>

instruction. This means textual instructions and images are implicitly associated via the design of Image Indicator Embeddings.

**Emu Edit Benchmark.** We also conduct a comparison on Emu Edit benchmark (Sheynin et al., 2024). It includes 3,589 examples of 8 tasks: background alteration, comprehensive image changes, style alteration, object removal, object addition, localized modifications, color/texture alterations, and text editing. This benchmark measures the similarity between output and input images and the provided captions. We calculate the L1 distance, CLIP similarity, and DINO similarity between the generated image and input image, together with the CLIP text-image direction similarity measuring agreement between the change in captions and the change in images, and CLIP similarity between the generated image and output caption. We use the code adapted from the MagicBrush evaluation code and models of CLIP ViT-B/32 and DINO ViT-S/16. As shown in Tab. 5, ACE achieves comparable performance to its baselines.

**Facial Editing.** When evaluating the face identity preservation ability, we designed a Face Similarity (FS) metric to measure the consistency of faces between generated images and original images. We first detect the face region using MTCNN (Zhang et al., 2016b), then extract face embeddings with the ArcFace (Deng et al., 2019a) algorithm. The cosine similarity between normalized embeddings is calculated as the face similarity score. The images generated by MagicBrush and InstructPix2Pix exhibit excessive similarity to the original images, thus metrics for these two methods are not computed. We observed a non-linear growth in the Face Similarity score. To analyze this, we extracted facial features from over 5 million data points in MS1M.V3 (Deng et al., 2019b) and grouped them into clusters based on their face\_id. We then calculated the pairwise similarity within each cluster, resulting in a mean of  $mean = 0.5258$  and a standard deviation of  $std = 0.1765$ . Due to the large standard deviation, we further analyzed the percentage of samples with scores above  $0.3493(mean - std)$  that met the instructions to evaluate the Effective Score(ES) of facial ID persistence.

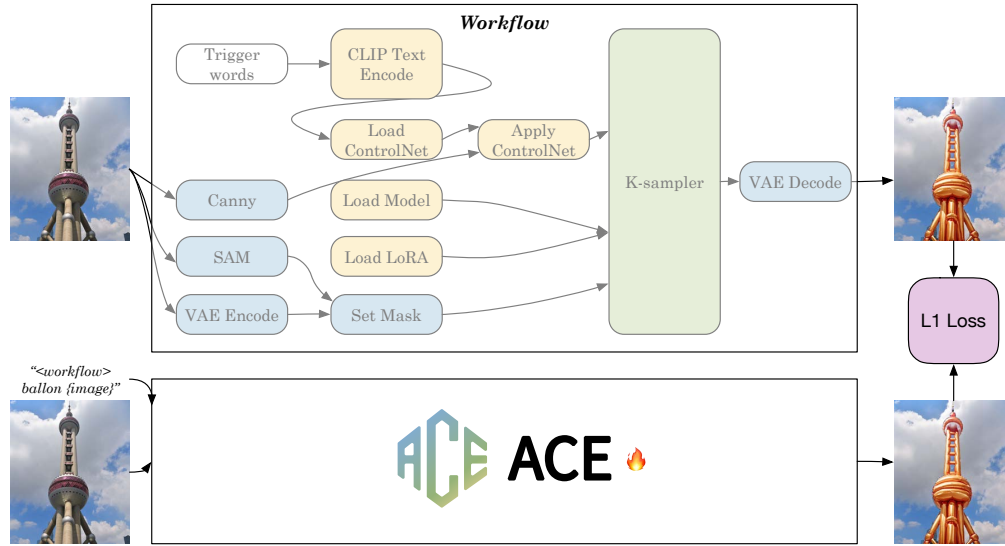


Figure 26: The pipeline of workflow distillation.

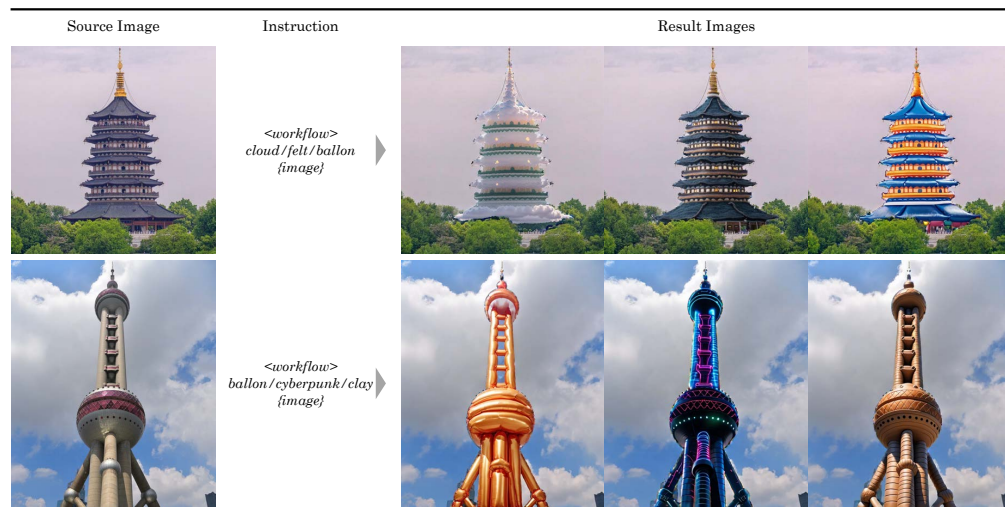


Figure 27: The results visualization of workflow distillation.

Our model significantly outperforms other methods in the absence of facial landmark information, with improvements of **3.56%** and **25%** in the FS and ES metrics as shown in Tab. 6. Although our model (0.6B) demonstrates inferior performance on metrics compared to InstantID (2.6B), it is important to highlight that InstantID utilizes an additional facial landmark as a conditioning factor. Moreover, as indicated by the results of prompt-following and image quality assessments in Tab. 2, our model shows a highly competitive performance overall.

**Local Text Render.** To adequately evaluate the performance of text editing, we provide the quantitative analysis of our method with two SOTA text render methods, *i.e.*, UDiffText, and Anytext, on the local text render task of ACE benchmark. Each generated text line is cropped according to the specific position and fed into an OCR model to obtain predicted results. As described in Anytext, we calculate the Sentence Accuracy and the Normalized Edit Distance for each method. The former metric evaluates the sentence-level accuracy and the latter metric evaluates the char-level precision. From Tab. 7 we can observe that our ACE outperforms the other two methods, achieving performance gains of **14%** and **16%** in terms of Normalized Edit Distance and Sentence Accuracy, respectively. This demonstrates our superior text rendering capability.

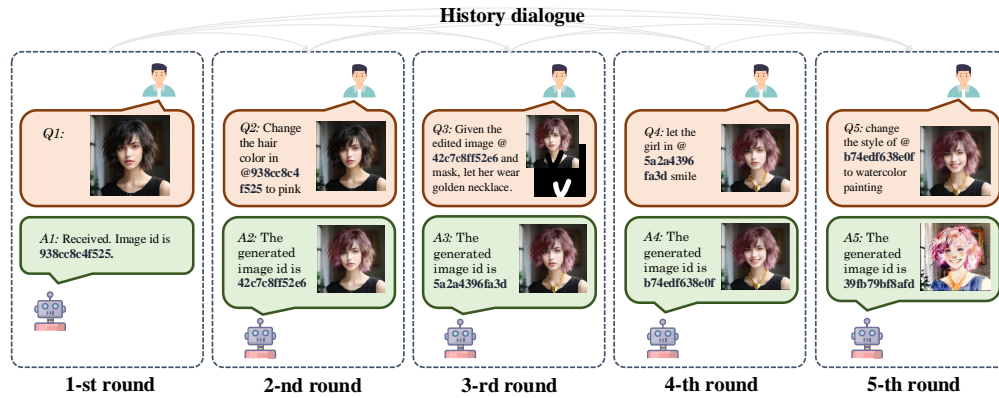


Figure 28: The multi-turn conversation pipeline of our chat bot application.

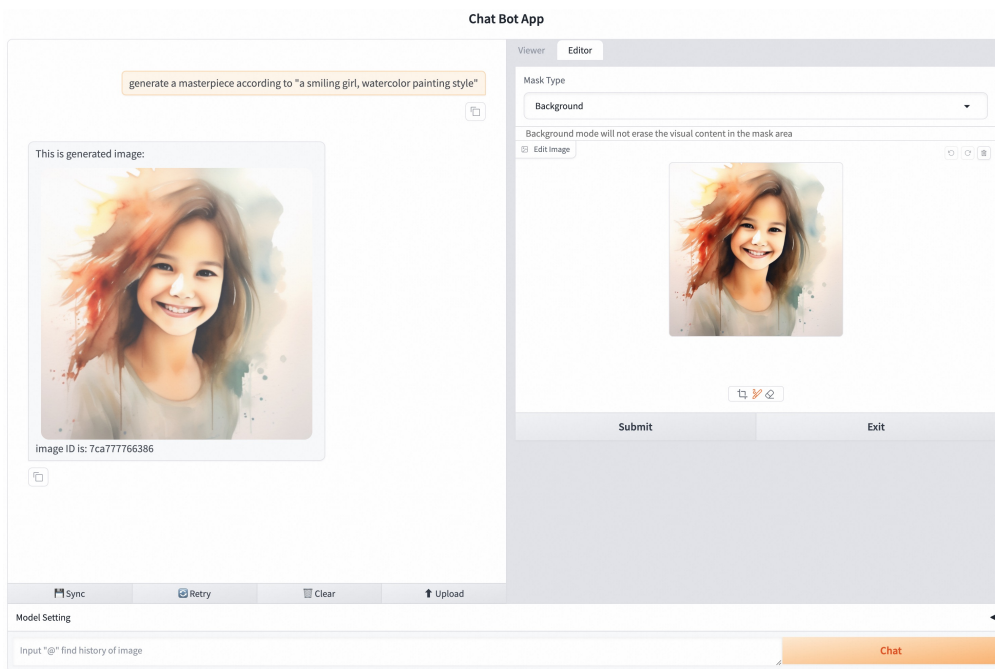


Figure 29: The user interface of the chat bot application built with Gradio.

## F APPLICATION

### F.1 WORKFLOW DISTILLATION

There are many excellent workflows assembling LoRAs, ControlNets, and T2I models on open-source platforms, which enable users to achieve certain results. To show the capability and compatibility of ACE, we collect several outstanding workflows to obtain their result images for distillation. We train ACE with the inputs and corresponding outputs of these workflows, as well as a fixed special trigger instruction, as illustrated at Fig. 26. Our model acquires similar abilities of these workflows, as shown in Fig. 27, which demonstrates the great potential of ACE.

### F.2 CHAT BOT

Leveraging our diffusion model, we build a chat bot application to achieve chat-based image generation and editing. Rather than a cumbersome visual agent pipeline, our chat bot supports all image creation requests with only one model serving as the backend, hence achieving significant efficiency improvement compared with visual agents. We depict a multi-turn conversation sample in 28 and

illustrate the user interface in Fig. 29. We could command the model to create any desired image by chatting with it using natural language. The overall system can be formulated as

$$A_j = ChatBot(H_{<j}, Q_j), \tag{6}$$

where  $A_j$  denotes the  $j$ -th round output of chat bot,  $Q_j$  represents the  $j$ -th round user request, and  $H_{<j} = \{(Q_1, A_1), (Q_2, A_2), \dots, (Q_{j-1}, A_{j-1})\}$  represents the history of dialogue before  $j$ -th round. By introducing the history dialogue information into the current conversation, our model excels at understanding complex user requests, therefore achieving better prompt following ability.

## G MORE VISUALIZATION

In Fig. 30, and Fig. 31, we present the visualization results of ACE in low-level visual analysis. The Fig. 32, Fig. 33, and Fig. 34 are the visualization of controllable generation. The visualization results of repainting are depicted in Fig. 35. Semantic editing tasks such as general editing, facial editing, and style editing are illustrated in Fig. 36, Fig. 37, Fig. 38. The visualization results of elements editing including text editing, and object editing are shown in Fig. 39, and Fig. 40. In Fig. 41, we present the visualization results of layer decouple and layer fusion. The visualization of reference generation can be found at Fig. 42 and that of multi-turn and long-context generation are present in Fig. 43. ACE demonstrates proficient instruction following, high-quality generation, and versatility across different tasks.

## H DISCUSSION

### Societal Impacts.

From a positive perspective, the intelligent generation and editing of images can provide artists and designers with innovative tools to inspire new concepts, enhance creativity and artistic expression in images, lower the barriers to artistic creation, and reduce the labor-intensive manual processes involved. Additionally, the method can serve various industries. In the field of education and training, they can be used to create supplementary teaching materials, such as illustrations for picture books, enhancing students’ learning experiences and improving communication and understanding in lessons. In business environments, companies can utilize the method to generate marketing materials and product designs, thereby increasing production efficiency and creative output. The positive impacts of these technologies offer new possibilities for creativity, educational quality, and business efficiency, making it worthwhile for us to actively explore and apply them.

New technologies not only bring new opportunities but also come with challenges. Firstly, issues related to copyright and authorship are prominent, potentially infringing upon the rights of original works and leading to legal disputes. Secondly, false information generated by models may exacerbate the spread of rumors, undermining public trust in information. Lastly, the inherent biases and stereotypes present in generated content can challenge societal values and moral standards. Therefore, while we acknowledge the conveniences and innovations offered by these technologies, it is imperative to carefully consider and effectively manage these negative impacts to ensure the sustainability of technological development and uphold social responsibility.

### Limitations.

First, our approach offers a unified framework for existing editing tasks. For specific tasks such as text-to-image generation, the aesthetic quality of our generated results lags behind that of state-of-the-art generative models like Midjourney and FLUX. These models have achieved breakthroughs by focusing on a single task of generating images from text prompts. In contrast, our model supports a broader range of input types and handles a wider variety of tasks, such as performing diverse edits under open-ended instructions. Additionally, training on higher-quality data and using a larger-scale model could help bridge this gap.

Second, the model for instruction editing needs to accurately capture the user’s actual intent. In our framework, we utilize a fixed encoder-decoder language model to encode text instructions. However, as user instructions become more complex and diverse, the difficulty of interpreting these instructions also increases. Furthermore, the current model is unable to handle multiple intents or tasks from a single instruction simultaneously and requires intent decomposition.

Third, we support the input of multiple images and multiple instructions to construct long contextual information for generation. On one hand, it is inevitable that, due to limited hardware resources, training and inference with multiple images become increasingly challenging as the number of tokens increases. On the other hand, excessively long contextual inputs pose a significant challenge for the model, as the forgetting of historical information during the process may lead to biases in the final generated results.

#### **Future Work.**

We try to illustrate some existing constraints of the model in limitations, which can serve as directions for our future work. Firstly, the phenomenon of scaling laws has been demonstrated in the NLP field, indicating that further exploration of scaling laws in complex generation tasks is warranted. We will focus on two main approaches: on one hand, we will work on expanding high-quality data, which includes improving data quality, incorporating more complex tasks, and enhancing the precision of instructional data; on the other hand, we will directly increase the model architecture's scale to enhance its general generative capabilities. Secondly, we aim to introduce LLMs or MLLMs to accurately capture the intentions of users at the instruction level, leveraging their robust general understanding of language and images. This involves two specific objectives: firstly, to enhance the model's ability to generalize from input text instructions to match single-task or multi-task contexts; and secondly, to improve the understanding of input images that are to be edited, thereby assisting subsequent instruction operations and ensuring the accuracy and diversity of the generated content. Finally, it is essential to explore the long-sequence modeling of multi-modal data comprising multiple rounds of image and text interactions. We will engage in continuous contemplation regarding how to ensure that the historical context of image-text pairs is truly beneficial, similar to the functionality of chatGPT-like language models.

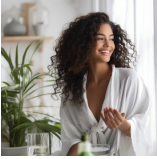











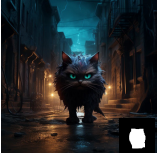




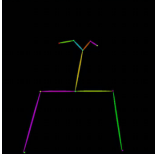
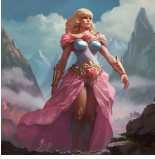
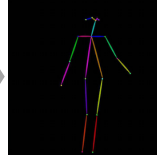

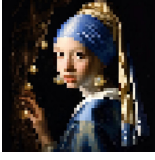
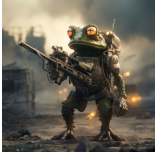
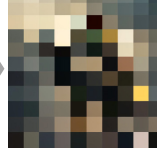

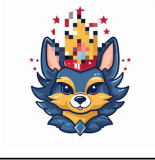
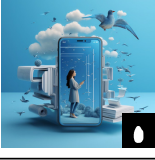



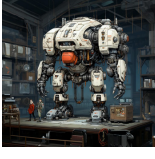
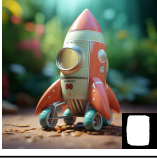

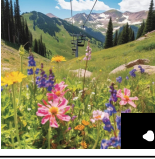

Image Segmentation	<p>Input Image</p> 	<p>Instruction</p> <p>Conduct a segmentation task on [image].</p>	<p>Output Image</p> 	<p>Input Image</p> 	<p>Instruction</p> <p>Set off with the segmentation of [image].</p>	<p>Output Image</p> 
	<p>Input Image</p> 	<p>Instruction</p> <p>Do segmentation on mask of [image].</p>	<p>Output Image</p> 	<p>Input Image</p> 	<p>Instruction</p> <p>Execute segmentation on mask in [image].</p>	<p>Output Image</p> 
Depth Estimation	<p>Input Image</p> 	<p>Instruction</p> <p>Produce a depth map for [image] please.</p>	<p>Output Image</p> 	<p>Input Image</p> 	<p>Instruction</p> <p>I need a depth map created from [image].</p>	<p>Output Image</p> 
	<p>Input Image</p> 	<p>Instruction</p> <p>Can you decipher the depth map from the portion of [image] highlighted by mask?</p>	<p>Output Image</p> 	<p>Input Image</p> 	<p>Instruction</p> <p>Generate the depthed depiction of the specified area in [image] as indicated by mask.</p>	<p>Output Image</p> 
Human-pose Estimation	<p>Input Image</p> 	<p>Instruction</p> <p>Can you help distinguish the poses of the figures in [image]?</p>	<p>Output Image</p> 	<p>Input Image</p> 	<p>Instruction</p> <p>Can you provide insight into the pose of the person presented in [image]?</p>	<p>Output Image</p> 
	<p>Input Image</p> 	<p>Instruction</p> <p>Adapt [image] into a mosaic representation.</p>	<p>Output Image</p> 	<p>Input Image</p> 	<p>Instruction</p> <p>Can we get a mosaic version of [image]?</p>	<p>Output Image</p> 
Image Mosaic	<p>Input Image</p> 	<p>Instruction</p> <p>Manipulate [image] to include mosaics in the sections specified by the mask.</p>	<p>Output Image</p> 	<p>Input Image</p> 	<p>Instruction</p> <p>Incorporate a mosaic into the [image], specifically in the mask regions.</p>	<p>Output Image</p> 
	Image Grayscale	<p>Input Image</p> 	<p>Instruction</p> <p>Can you transform [image] into a black and white one?</p>	<p>Output Image</p> 	<p>Input Image</p> 	<p>Instruction</p> <p>Could you adjust [image] to be black and white?</p>
<p>Input Image</p> 		<p>Instruction</p> <p>Would you mind converting the mask section of the [image] into a monochrome hue while keeping the rest as it is?</p>	<p>Output Image</p> 	<p>Input Image</p> 	<p>Instruction</p> <p>Could you please transform the mask area of the [image] into grayscale, while leaving the rest as per original?</p>	<p>Output Image</p> 

Figure 30: The ACE's generated visualization of image segmentation, depth estimation, human-pose estimation, image mosaic, and image grayscale in low-level visual analysis.



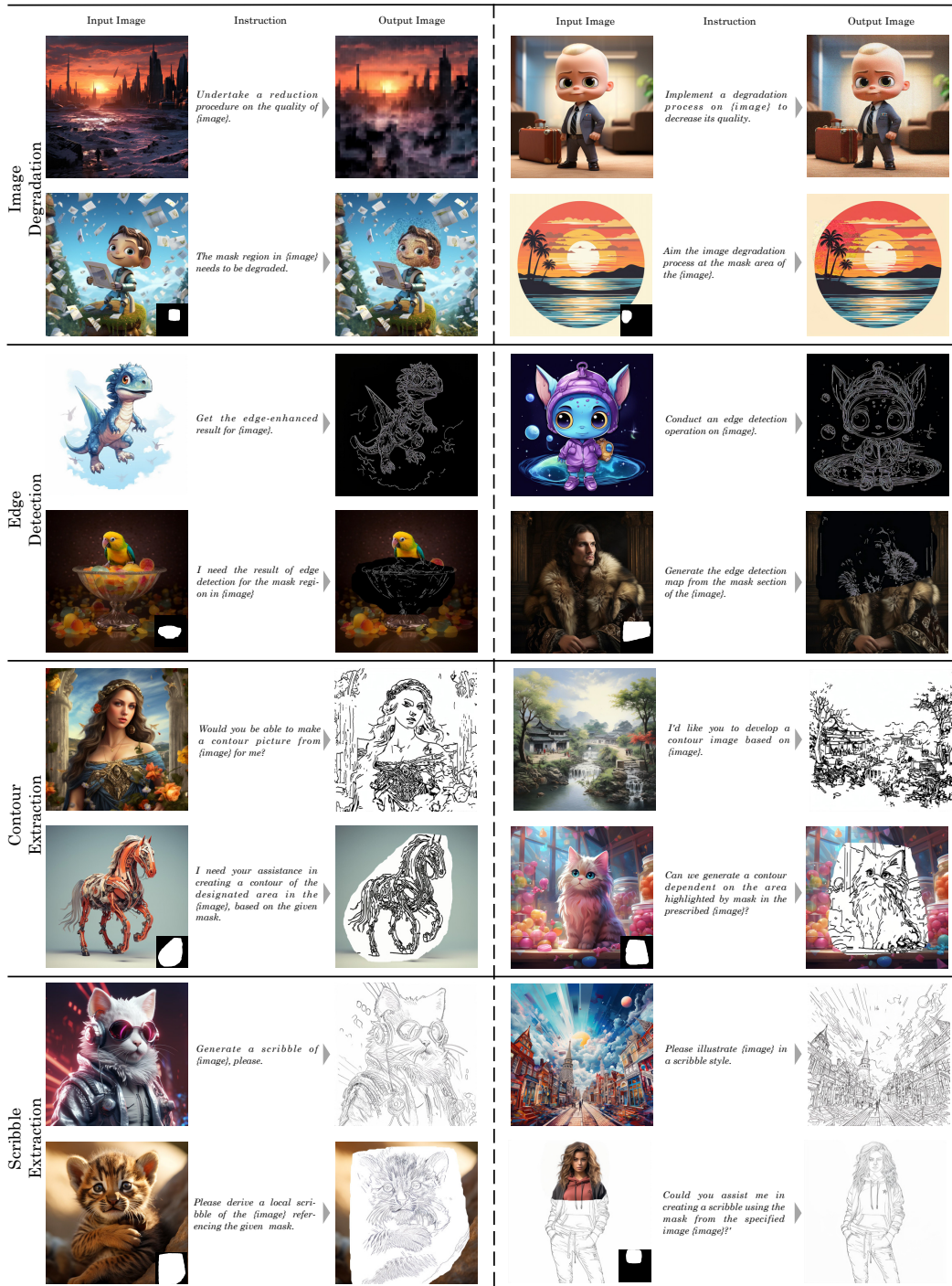


Figure 31: The ACE's generated visualization of image degradation, edge extraction, contour extraction, and scribble extraction in low-level visual analysis.

	Input Image	Instruction	Output Image	Input Image	Instruction	Output Image
Segmentation-based Generation		Based on the primitives from [image], synthesize a real image that fits the context and details provided in "a charming girl, long black straight hair, sky background, in yuumei style, realistic portrait".			"rugged man wearing aviator sunglasses on deep red background", Transforming [image]	
		Following the segmentation outcome in mask of [image], develop a real-life image using the explanatory note in "water-colour, dreamy, stuido ghibli, art nouveau".			"Character design sheet of a asian woman, round face, round spectacles, messy cute hair, freckles, small nose, white background", Develop a detailed image from the image segmentation represented by mask of [image].	
Depth-based Generation		Could you use the depth map and the text caption "a young elf-like character with pointed ears, green eyes, and blonde hair, adorned in a red and brown outfit with green accents. A bokeh effect with green hues and hints of light reflecting through foliage" to create a corresponding graphic image?			Create character reference illustrations of Oliver, an adventurous 8-year-old, has tousled brown, wind-blown, outdoor lifestyle, hazel eyes, freckles. Oliver wears, worn green adventurer, vest", Could you bring to life an image using the depth map [image]?	
		A cartoon dinosaur, likely a Tyrannosaurus Rex, dressed in a white astronaut suit, set against a backdrop of outer space. The dinosaur is colored in vibrant shades of orange, with a lighter shade on its underbelly. Please restore the region of the photo highlighted by mask using the information from the depth map [image].			"A close-up illustration of a penguin wearing large, orange sunglasses. The sunglasses have a thick, orange frame and dark blue lenses that reflect the penguin's surroundings.", Utilizing the depth map [image], I'd like you to reestablish the local zones as indicated in mask.	
Pose-based Generation		Could you please help translate this posture schema [image] into a colored image based on the context I provided "dwarf character dungeons & dragons with blue eyes, long barb and mustache, total body"?			I'm hoping to turn this pose guide [image] into a full color image with your help, using my description provided in the "a cartoon-style eagle dressed in a black leather jacket, round sunglasses, a feathered chest piece, and accessorized with a necklace and earrings".	
Mosaic-based Generation		Transform and generate an image using mosaic [image] and "Osamu Tezuka middle aged astro man" description			A woman representing the herb lavender, photorealistic, beautiful, detailed, Could you bring back the integrity of this mosaic art [image] by transforming it into its original photograph?	
		A whimsical, steampunk-inspired goldfish, a fascinating fusion of transparent glass and gleaming metal, reveals an intricate network of gears, pipes, and wires, hinting at a complex internal mechanism. Would you be able to eliminate the mosaic in areas indicated by mask on [image] to uncover the underlying image part.			Several wooden balconies adorn the exterior of the treehouse, each lined with potted plants and small windows.", Recover the image [image] by taking away the mosaic on the mask area.	
Grayscale-based Generation		Can you make this [image] colorful as per the "retrofuturism exploration on mars"?			"Futuristic robotic astronaut floating, dynamic posture, with a sense of design, cartoon style, cartoon astronaut, cartoon proportions, anime aesthetics, with ultra fine textures, with ultra fine textures, 3D, black background", Please transform this grayscale [image] into full color.	
		Make the mask part of my [image] to be color processed based on the notes "a whimsical, steampunk-inspired airship, seemingly cobbled together from various salvaged parts. It's a vibrant orange and white, with exposed pipes, gears, and wires adding to its ramshackle charm".			The chimpanzee is wearing a yellow astronaut helmet, and its head and shoulders are visible. The chimpanzee's fur is black and its eyes are brown. Its mouth is slightly open, and its teeth are visible. Kindly apply color to the mask portion of the [image], while the rest of it stays in grayscale.	

Figure 32: The ACE's generated visualization of segmentation-based, depth-based, pose-based, mosaic-based, and grayscale-based generation in controllable generation.



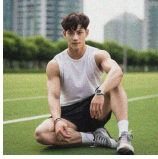



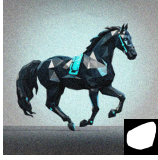
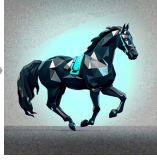
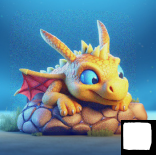
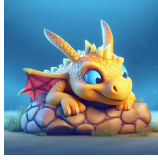

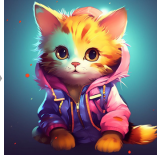

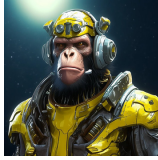


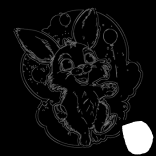


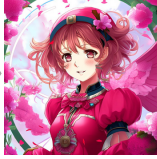

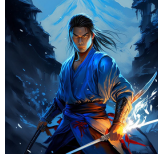
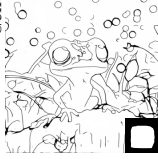


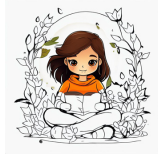

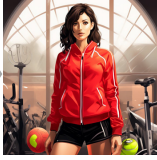

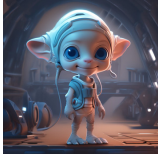
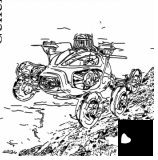




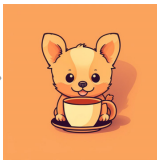

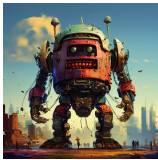
Degradation-based Generation	<p><b>Input Image</b></p> 	<p><b>Instruction</b></p> <p>"Handsome boy, age 20 years old, chest and gluteal muscles developed, six pack abs, white sports shorts, smile, short hair, less chest hair, white sports shoes, sitting on the grass". Eliminate noise interference in [image] and maximize the crispness to obtain superior high-definition quality.</p>	<p><b>Output Image</b></p> 	<p><b>Input Image</b></p> 	<p><b>Instruction</b></p> <p>Adhere to "Ultra clear, high resolution, high detail, Chinese style, Ancient Chinese, face view, long black hair, brown eyes, frontal, horizontal Angle, facing camera, outdoor, street, serious, upper body" to clean the noise from [image] and develop a clearer visual.</p>	<p><b>Output Image</b></p> 
	<p><b>Input Image</b></p> 	<p>The horse stands against a gradient background that ranges from light to dark, emphasizing the contrast of the horse's colors. The background could be interpreted as either the light of day or the darkness of night, depending on the viewpoint of the observer". Denoise the mask segment in the [image] to improve clarity.</p>	<p><b>Output Image</b></p> 	<p><b>Input Image</b></p> 	<p>The dragon is yellow with orange accents, featuring spikes along its back and spikes on each cheek. Its eyes are large and bright blue, adding to its expression of contentment. Execute high resolution refinement on the mask area of the [image].</p>	<p><b>Output Image</b></p> 
	<p><b>Input Image</b></p> 	<p>Take the edge conscious [image] and the written guideline "cat wearing colorful shirt, brown eyes, bright brown eyes, chibi, detailed fur", high resolution, 4k, soft fur" and produce a realistic image.</p>	<p><b>Output Image</b></p> 	<p><b>Input Image</b></p> 	<p>"Create a cybernetic monkey character positioned at a 45-degree angle, existing within the vast expanse of the universe. The monkey wears a sleek yellow-trimmed suit adorned with futuristic elements and one earring in the ear.". Craft a genuine image by leveraging the edge representations in [image].</p>	<p><b>Output Image</b></p> 
	<p><b>Input Image</b></p> 	<p>The head of the robot mimics a large, white, cartoon-like animal with a simple smiling face, featuring large expressive eyes and minimal design features like a cute nose and a small triangle shape for the mouth.". Interpret the aspects of the mask region in the [image] into an authentic image</p>	<p><b>Output Image</b></p> 	<p><b>Input Image</b></p> 	<p>Rebuild a lifelike image by using the edges of [image] under the guidance of the mask.</p>	<p><b>Output Image</b></p> 
Doodle-based Generation	<p><b>Input Image</b></p> 	<p>"Card captor sakura". Please instruct on creating an equivalent image of the doodle [image].</p>	<p><b>Output Image</b></p> 	<p><b>Input Image</b></p> 	<p>"A young man with glowing eyes, hair in a pony tail, epic pose, holding a blue flame Katana, GLOWING samurai armor, in the mountains, painterly style". Create an image that accurately represents the doodle depicted in [image].</p>	<p><b>Output Image</b></p> 
	<p><b>Input Image</b></p> 	<p>Create a regional image from the doodle [image], based around the text descriptor "A bright blue, anthropomorphic frog is depicted with a large, expressive eye and several smaller protrusions on its skin." marked by the mask.</p>	<p><b>Output Image</b></p> 	<p><b>Input Image</b></p> 	<p>Please provide me with instructions on how to regenerate a portion of the doodle [image] that matches with the description "A young girl with brown hair wearing an orange hoodie." from the masked area mask.</p>	<p><b>Output Image</b></p> 
Contour-based Generation	<p><b>Input Image</b></p> 	<p>An artistic illustration of a woman in a bright red jacket and black shorts stands prominently in front of a semi-transparent wall. Behind her, there are gym equipment and what appears to be the silhouette of a tennis court. For the contour [image], create a suitable matching image.</p>	<p><b>Output Image</b></p> 	<p><b>Input Image</b></p> 	<p>Please follow the description "a 3D digital art style image of an animated child character, showing a alien child in a space suit.His expression was friendly, and his eyes showed curiosity and excitement". Process the contour map [image] and output the appropriate image.</p>	<p><b>Output Image</b></p> 
	<p><b>Input Image</b></p> 	<p>The vehicle is a futuristic concept with a sleek, rounded design, featuring multiple rotors for lift and propulsion. Its exterior is primarily an iridescent orange, with details that suggest advanced materials and technology. By amalgamating the contour image [image] we can produce a localized image in the mask mask area.</p>	<p><b>Output Image</b></p> 	<p><b>Input Image</b></p> 	<p>Using the specified mask region and taking "a charming, whimsical stone house, seemingly plucked from a fairytale. The house is constructed from large, unevenly shaped, light brown stones" as the reference, create an image partial corresponding to the [image] contour.</p>	<p><b>Output Image</b></p> 
Scribble-based Generation	<p><b>Input Image</b></p> 	<p>"A cute little brown and white dog with erect ears and playful mouth. He's enjoying his coffee and looks like he's enjoying it.". please create the corresponding local image in the [image] draft according to the area indicated by mask.</p>	<p><b>Output Image</b></p> 	<p><b>Input Image</b></p> 	<p>"A robotic monster by Edmund McMillen". Could you please generate the image that corresponds to the given scribble [image]?</p>	<p><b>Output Image</b></p> 

Figure 33: The ACE's generated visualization of degradation-based, edge-based, doodle-based, contour-based, and scribble-based generation in controllable generation.

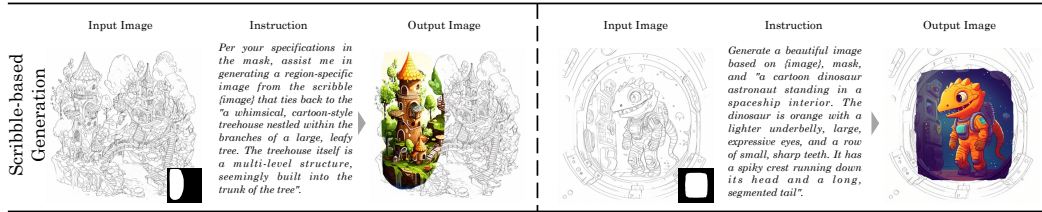


Figure 34: The ACE’s generated visualization in scribble-based controllable generation.

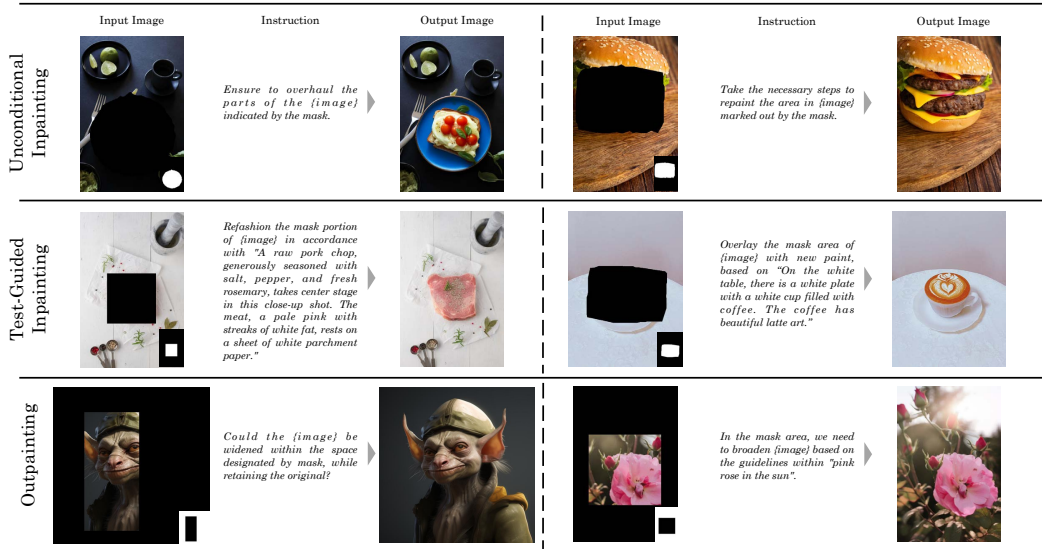


Figure 35: The ACE’s generated visualization of repainting.

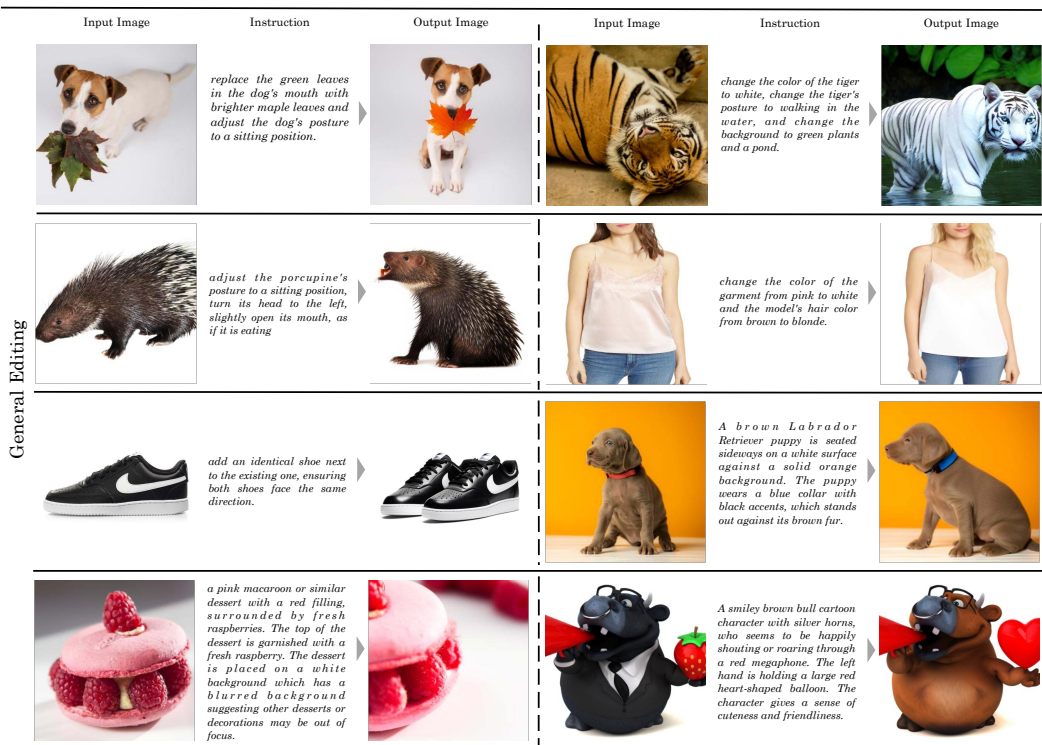


Figure 36: The ACE’s generated visualization of general editing in semantic editing.



	Input Image	Instruction	Output Image	Input Image	Instruction	Output Image
Facial Attributes Preservation		Maintain the same face in [image], you need to revert the background to a clear indoor or shaded setting, using bright lights and increasing contrast. The clothing can be adjusted back to a large ruffled white garment or jacket, maintaining its original style.			Restyle the characters from [image] according to "the woman has straight, light brown hair with a side part, which is swept away from her face. She is wearing a white top with cut-out details, and her makeup appears more natural." and make sure their facial attributes remain the same.	
		You need to change the background color from pink elements and stairs or step patterns to a blurry background with a repeating pattern. Remove the shadows and restore the soft glow atmosphere. Also, adjust the background color back to blue. The faces in the two images are the same, usually changing their pose.			Modify the [image] as per the "has her hair flowing more dynamically, suggesting movement or a breeze, and the background has more defined greenery, creating a natural and serene setting. The light is more diffuse and the color tones are rich, which adds to the realistic feel of the scene." while preserving facial identity.	
		Replace the long-sleeved blouse with a high neckline featuring a pattern of red chains against a pale background with a sleeveless top with lace detailing at the straps. Additionally, the large hoop earrings and textured clutch purse should be replaced with a broad smile.			Correspond the composition of [image] with another style taking into account the "The girl has a light blue, long-sleeved shirt with a floral pattern, which seems comfortable and casual. The setting is outdoors, with greenery softly in the background." but keeping the facial aspects constant.	
		Decrease light on the well-lit side to create appropriate shadows. Conceal some parts of the shoulder and arm. Also, adjust the stripe pattern on the collar edge. The faces in the two images are the same, usually changing their pose.			Keep the same facial feature in [image], change the woman's clothing from a white jacket to a white turtleneck sweater and adjust her posture so that she is pulling the collar of the sweater with both hands. Other aspects, such as background, hairstyle, facial expression, etc., remain unchanged.	
		Keep the facial features of the character in [image], based on "change the background to solid pink. Turn the character's shirt black, change their hairstyle to short hair, and make their gaze more determined."			Keep the same facial feature in [image]. Transform the girl's outfit into a formal dress with suspenders, spread her hair out, and hold a large bouquet of red roses in her hand. The overall lighting becomes dim, creating a sense of atmosphere	
		Transform the faces of the character in [image] to capture genuine smiles.			Adjust the expressions of the character in [image] to reflect natural, friendly smiles.	
		The person appears to be wearing more subtle makeup to enhance his facial features. The skin appears to be smoother, with possibly a touch of foundation to even out the complexion. A light application of blush might have been used to give a healthy glow to the cheeks.			The person in [image] is wearing makeup. The makeup enhances the lips, making them appear fuller and more vivid. The eyebrows are neatly shaped with color added, while the skin looks smoother and perhaps given a lighter tone from the makeup application.	
		Add natural beards to the characters in the [image].			Generate natural facial hair for the character in the [image].	
		The character's hair color appear as vibrant pink, with the same styled bun and loose tendrils framing her face. The character continues to wear the same clothes and accessories. The makeup remains largely unchanged, focusing attention on her facial features.			The woman's hair has transformed to a deep purple hue, with a more pronounced wave similar to that in the left image. The length and style appear to be the same as the left image. The overall effect is still soft and ethereal, but distinctly different in the hair color.	

Figure 37: The ACE's generated visualization of facial editing in semantic editing.





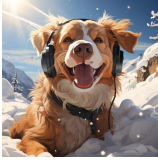
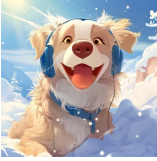




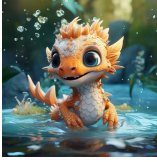
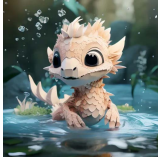
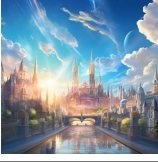

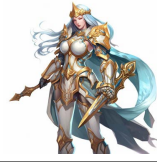


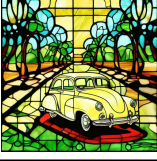
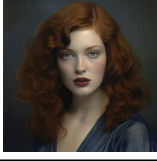



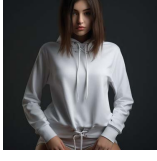
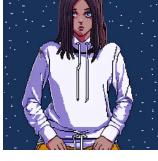
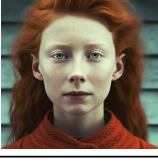





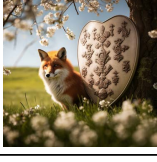
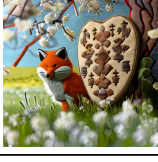
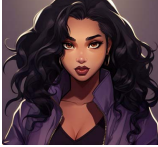
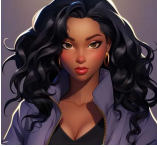


	Input Image	Instruction	Output Image	Input Image	Instruction	Output Image
Schools of Painting		Could you please make [image] an Impressionism painting.			Let [image] be in the style of Fauvism.	
Animation Studios		Create a new image of Walt Disney Animation referring to [image].			Adjust the [image] to capture the essence of Ghibli Studio's style.	
Paper Art		Change the style of [image] to paper cut craft.			Convert [image] into a paper cutting.	
Drawing		Transform [image] into pencil painting.			Give [image] a one line drawing look	
Materials		Make [image] a picture made of stained glass			Make [image] in Play-Doh clay style	
Special Effects		Change [image] to match Low poly style.			Change [image] to match 8-bit pixel art style	
		Re-style [image] to risograph ISO format			Make [image] in ink render style	
Fabrics		Apply felt doll style to [image].			Generate a quilted art style image using the [image] content.	
3D		Could you please make [image] 3D cartoon.			Make [image] a Pixar Animation.	

Figure 38: The ACE's generated visualization of style editing in semantic editing.



	Input Image	Instruction	Output Image	Input Image	Instruction	Output Image
		On the (image), superimpose the text "LAKE" according to the area identified by the mask			Put the text "CARD" at the position marked by mask in the (image)	
		Embed the text "EVER" in the (image) at the location indicated by mask			By using the mask as a guide, you can position text "RPG" on (image)	
Text Render		Stamp text "FRIDAY" into the (image), as defined by the mask coordinates			In the image (image), position the text "Food" according to the guidance of the mask	
		text "STRONG" should be applied to the (image) at the position marked by mask			The mask is to be used as a marker to incorporate the text "DANGEROUS" into the (image)	
		add white text 'UFES' near the center of the image.			add the light brown text 'NVZ' at the bottom right of the picture	
		Rub out any text found in the mask sector of the (image).			Obiterate the text from the specified mask slice of the (image)	
Text Remove		Vacate the text from the identified mask spot on the (image).			Obiterate the text in the mask in the (image) image	
		Aim to remove any textual element in (image)			Let's make the (image) completely devoid of any text	
		Scrub out every text snippet from (image)			Eradicate all text on (image)	

Figure 39: The ACE's generated visualization of text editing in element editing.



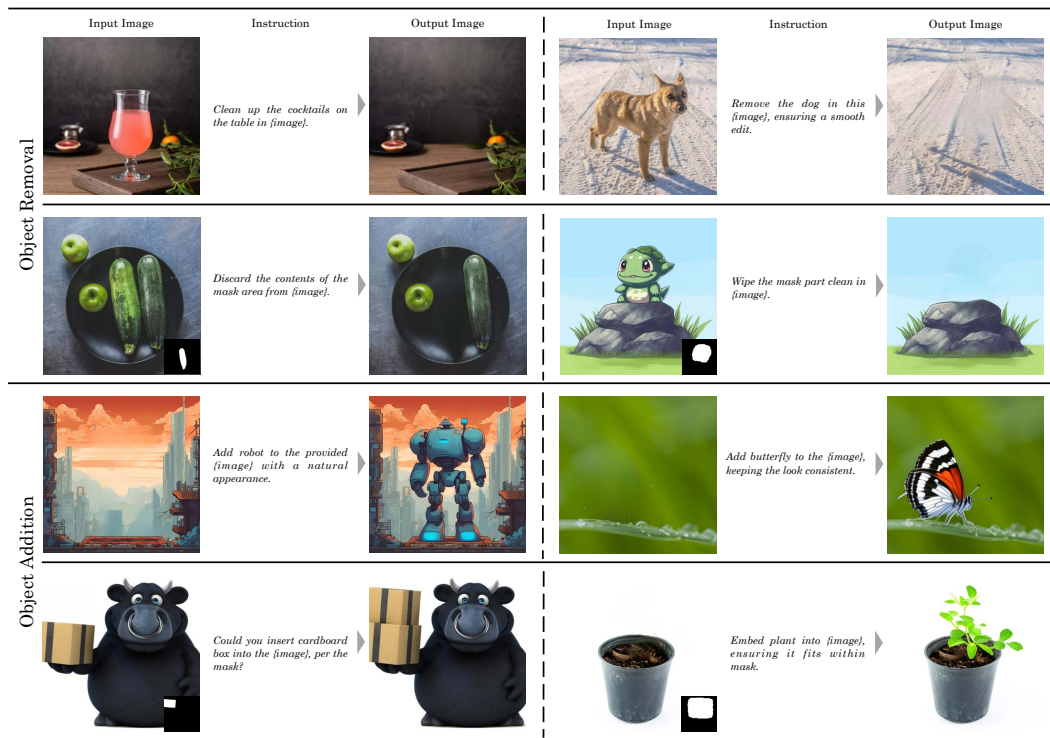


Figure 40: The ACE's generated visualization of object editing in element editing.

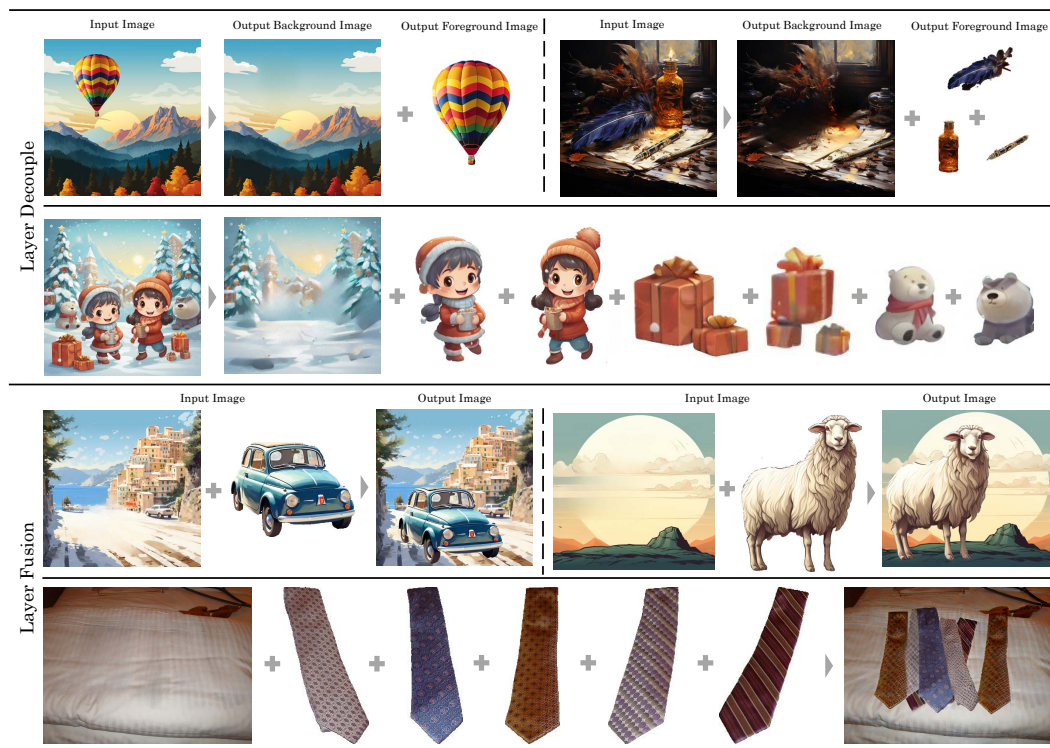


Figure 41: The ACE's generated visualization of layer decouple and layer fusion in layer editing.

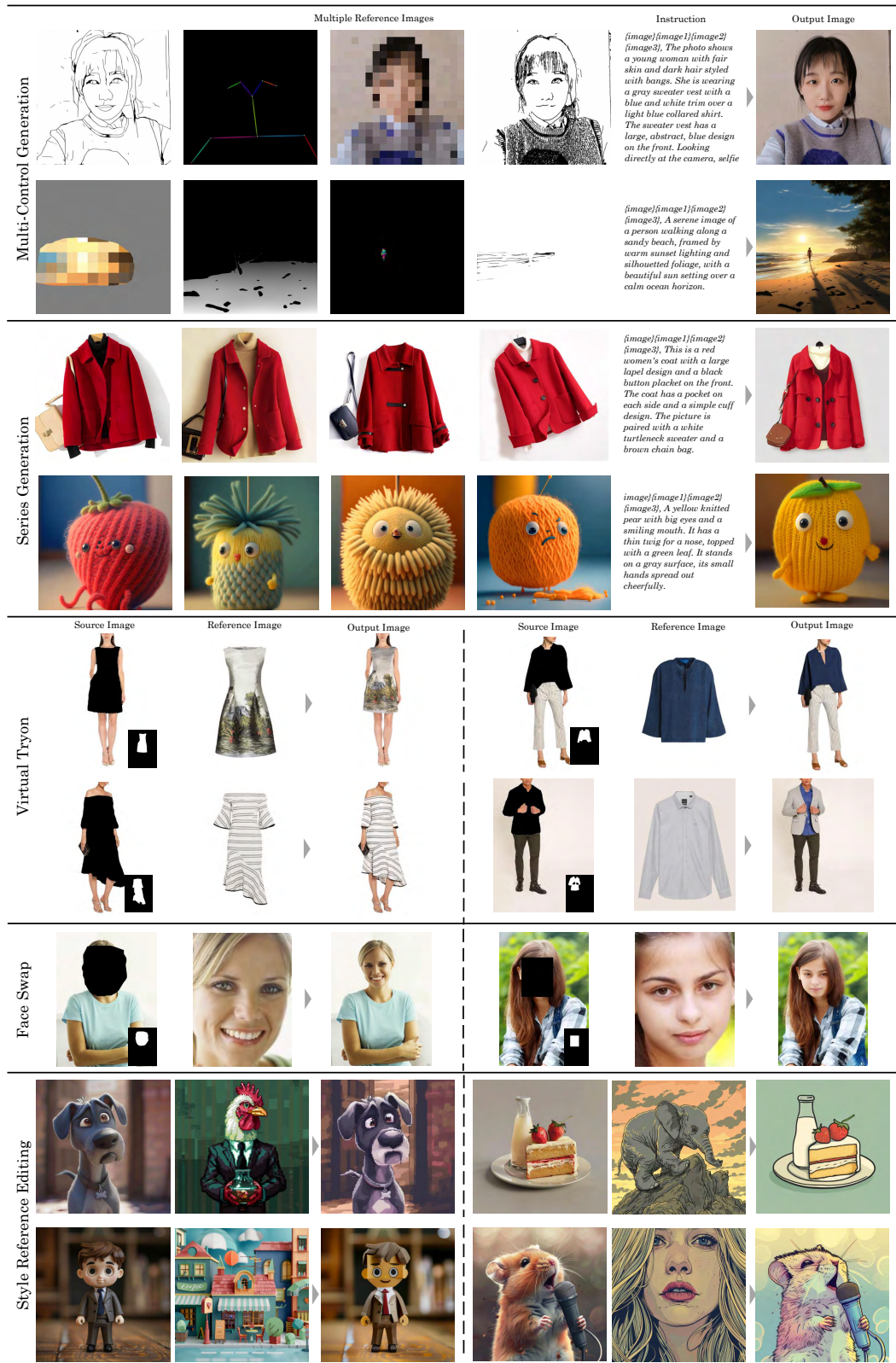


Figure 42: The ACE's generated visualization of multi-reference generation and reference-guided editing.



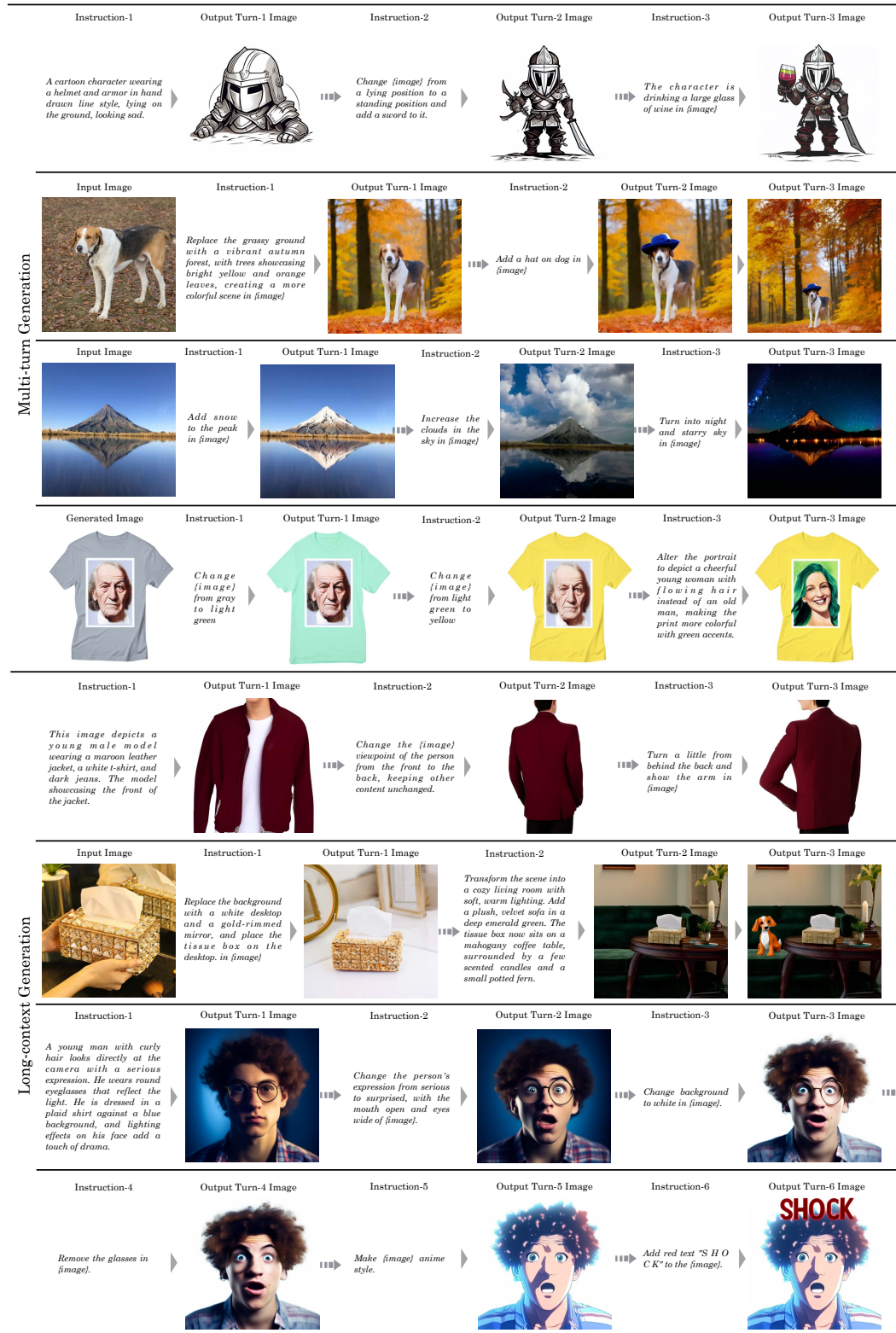


Figure 43: The ACE’s generated visualization of multi-turn and long-context generation.